JOURNAL OF GEOPHYSICAL RESEARCH, VOL. 93, NO. B9, PAGES 10,349-10,372, SEPTEMBER 10, 1988

SAN JACINTO INTRUSIVE COMPLEX
2. GEOCHEMISTRY

R. I. Hill[1]

Division of Geological and Planetary Sciences, California Institute of Technology, Pasadena

B. W. Chappell

Geology Department, Australian National University, Canberra

L. T. Silver

Division of Geological and Planetary Sciences, California Institute of Technology, Pasadena

Abstract. Rocks from three large (>100² km) tonalitic intrusions exposed in the San Jacinto Mountains of southern California show a restricted compositional range of between 63 and 68 wt % SiO_2 for all but volumetrically minor felsic differentiates (with SiO_2≈70 wt %). All rocks with less than 65.5 wt % SiO_2 show linear element-element covariation. Felsic differentiates have characteristics (higher SiO_2, K_2O, Rb, Ba, U; higher and variable rare earth elements) consistent with derivation by in situ fractionation; rocks with between 65.5 and 70 wt % SiO_2 have intermediate characteristics and are interpreted as derived from liquids formed by mixing "primitive" liquids with fractionated liquids within an intermittently recharged, continuously solidifying magma chamber. Mafic inclusions extend the compositional trends of the mafic tonalites to 55 wt % SiO_2. The chemical variations of both inclusions and more mafic tonalites are interpreted as resulting from processes acting before injection of their parental liquids into the observed crustal magma chambers. Effects of chamber processes are minor for all but the most felsic rocks. The major effect of recharge is to buffer the thermal and chemical properties of liquids within the magma chambers, yielding large volumes of relatively homogeneous tonalite. For those elements where the bulk distribution coefficient is between about 0.5 and 2, concurrent recharge and solidification produces rocks that closely approximate the composition of the added liquids. Estimated Rayleigh numbers for these liquids are high (>10^{10}), implying convection throughout much of the solidification history of each chamber. Existence of trace element variations within analyzed rocks imply that convection was not totally efficient at homogenizing the various batches of liquid added to each chamber.

Introduction

The chemical composition of an igneous rock is a complex function of the chemistry of its source volume, of the conditions prevailing during partial fusion, and of the effects of processes operating during magma collection, transport, and solidification. Even so, study of the chemistry of granitic rocks has had tremendous influence on the development of current theories of granite (in the broadest sense) genesis [e.g., Larsen, 1948; Presnall and Bateman, 1973; Chappell and White, 1974; White and Chappell, 1977; Compston and Chappell, 1979; Collins et al., 1982]. This work has demonstrated that granitic rocks may be derived by partial fusion of materials with a wide variety of compositions, including many crustal rock types, and that the composition of a granite reflects the composition of its source volume or volumes to some degree. Magma chamber processes may modify source-related characteristics, and it is toward the elucidation of the effects of such high-level processing that the work reported here is directed.

This paper reports new chemical data for both igneous and metasedimentary rocks from the San Jacinto Mountains of southern California and considers the geochemical effects of crystallization accompanied by episodic recharge in the dynamic magma chambers deduced from field observations [Hill, this issue; Hill et al., 1985]. A third paper in this series describes strontium isotope heterogeneties within these rocks and uses these data to further limit likely processes within these large crustal magma chambers [Hill and Silver, this issue].

The geology of the igneous rocks of the San Jacinto Mountains is described by Hill [this issue]. Briefly, three large (>100 km^2) and many small plutons intrude older heterogeneous igneous and metasedimentary rocks. The small early intrusives span the compositional range olivine gabbro to granite. Three younger major tonalites are composed of relatively homogeneous tonalite. Unit I was emplaced into igneous and quartz-rich metasedimentary country rocks; unit II was, in part, emplaced into unit I before complete solidification of the older unit, and unit III, in turn, was emplaced before complete solidification of unit II. Unit III is compositionally zoned from a mafic tonalite rim (color index >15) to a felsic tonalite or K-feldspar-poor granodiorite core (colour index ≈10). All igneous rocks were emplaced within a restricted time interval between 92 and 99 Ma (L.T. Silver et al., manuscript in preparation).

Dark mafic inclusions of quartz diorite or tonalite are common within the three major tonal-

[1]Now at Research School of Earth Sciences, Australian National University, Institute of Advanced Studies, Canberra.

Paper number 4B5361.
0148-0227/88/004B-5361$05.00

ites; dykes of similar composition are also found but are more common within the more mafic, commonly marginal rocks. Field observation suggests that dykes of tonalitic composition are volumetrically more significant than are quartz dioritic dykes; they are, however, difficult to distinguish from their mafic tonalitic host. In places, dykes appear to be being broken up and redistributed to form linearly extensive inclusion trains paralleling the pluton walls. This relationship has been interpreted as evidence that the dykes were conduits through which compositionally variable new material was intermittently added to an inflating and solidifying magma chamber.

This model for magma chamber inflation predicts considerable thermal and chemical buffering of liquids within the magma chamber by the episodic addition of new, hot, "primitive" materials. This is in accord with the considerable mineralogical and petrographic evidence for thermal and chemical buffering of the solidifying magma chambers described by Hill [1984, this issue].

Analytical Procedures

A total of 104 igneous (including six inclusions and two dyke rocks) and 11 metasedimentary rock samples from the San Jacinto Mountains have been analyzed for 11 major and 19 trace cations and for S, H_2O^+, H_2O^- and CO_2.

Approximately 500 g of rock chips randomly selected from a larger sample were powdered in a tungsten-carbide lined Spex-"Shatterbox." An aliquot of this powder was then analyzed by the methods of Norrish and Hutton [1969] and Norrish and Chappell [1977]. Major elements (Si, Ti, Al, Fe, Mg, Mn, Ca, K, S, and P) were determined by X ray fluorescence spectrometry of glass discs fused with lithium borate and doped with a La_2O_3 absorber [Norrish and Hutton, 1969]. Hygroscopic water (H_2O^-) was determined by weight loss at 110°C for 2 hours. H_2O^+ and CO_2 were determined by firing at 1200°C for 30 min in a stream of dry nitrogen followed by collection on P_2O_5 and "carbosorb" respectively. Ferrous iron was determined by titration of a boric-sulphuric-phosphoric acid buffered solution with potassium dichromate following sample digestion in warm HF-H_2SO_4 in a closed Pt crucible. Na was determined by flame photometry of an acidic solution using a Li internal standard. Trace elements (Ba, Rb, Sr, Pb, Th, U, Zr, Nb, Y, La, Ce, Nd, Sc, V, Cr, Mn, Ni, Cu, Zn, and Ga) were determined by XRF spectrometry on pressed powder pellets [Norrish and Chappell, 1977] using directly measured absorption coefficients for the heavier elements. Corrections are made for nonlinear backgrounds and interelement interferences. Limits of detection for each element are as outlined by Norrish and Chappell [1977] and precision for most elements is estimated to be better than ±5%.

Most of the samples for which Rb and Sr concentrations were determined by XRF spectrometry have had Rb and Sr determined by isotope dilution mass spectrometry [Hill and Silver, this issue]. Agreement for Sr is excellent, usually to better than ±2%. Analytical results for Rb are not quite as good; there appears to be a small unexplained interlaboratory bias between the two determinations, with the isotope dilution values being about 3% higher than those obtained by XRF.

Results

Chemical data for igneous rocks are listed in Tables 1-3. Sample locations are shown on Figure 1. The total range in SiO_2 for analyzed igneous rocks from the San Jacinto Mountains is 45.1-73.7 wt %, and demonstrates the wide variation present in the rocks of this area. The bulk of the rocks have a more restricted range in SiO_2, from 63 to 68 wt % SiO_2. Samples from the major tonalites form a geochemically coherent group with a much smaller range in chemistry than the more diverse early intrusives.

The metasedimentary country rocks are subdivided into the Desert Divide Group, a sequence of quartz-rich schists and gneisses containing a considerable quartzite component, and the Windy Point metamorphics, consisting of interlayered plagioclase amphibolites, amphibolites, meta-carbonates and quartzo-feldspathic schists and gneisses. The Desert Divide Group rocks are characterized by low CaO, reflecting their almost plagioclase-free nature, and high Al_2O_3 in the low-SiO_2 samples, a result of the clay-rich nature of their mature sedimentary protolith. These rocks also have high Zr contents (≈250-400 ppm). The Windy Point metamorphics, in contrast, were derived from very immature sediments, and this is seen in their high CaO and relatively Al_2O_3-poor compositions. Because work has been concentrated on the three major tonalite plutons, they will be discussed first.

Major Tonalites

Major elements. The three major tonalite units are chemically similar. SiO_2 in all three

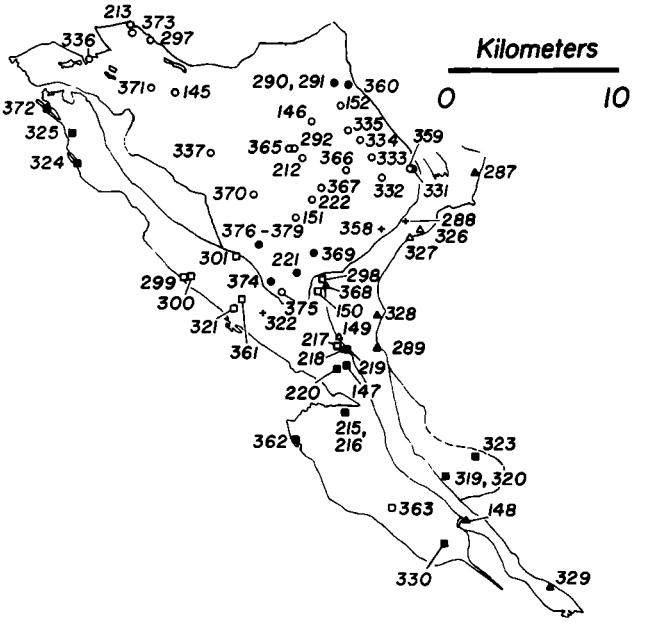

MAJOR TONALITES

Sample Localities

Fig. 1. Palinspastic base showing pre-San Jacinto fault configuration of San Jacinto Mountains and geochemistry sample locations. Palinspastic reconstruction after Hill [1984].

TABLE 1a. Major Tonalites

	Unit I															
	Tonalites and Granodiorites															
	LTS323	LTS215	LTS147	LTS319	LTS330	LTS220	LTS362	LTS325	LTS372	LTS324	LTS219	LTS150	LTS300	LTS299	LTS217	LTS321
SiO_2	62.53	62.91	63.27	63.65	63.83	63.93	64.10	64.21	64.57	64.63	65.05	65.57	65.66	65.69	66.11	66.11
TiO_2	0.95	1.01	0.95	0.90	0.95	1.03	0.84	0.81	0.72	0.87	0.83	0.72	0.74	0.75	0.68	0.66
Al_2O_3	17.07	16.75	16.76	17.16	16.72	16.60	16.56	17.33	17.09	17.15	16.10	16.70	16.57	16.43	15.65	16.57
Fe_2O_3	1.55	0.89	0.90	0.86	1.33	0.85	1.32	0.62	0.31	0.63	1.32	1.14	0.93	0.86	1.08	0.68
FeO	3.11	3.76	3.59	3.29	2.98	3.23	2.87	3.25	3.06	2.91	2.67	2.43	2.64	2.75	2.20	2.79
MnO	0.07	0.07	0.06	0.06	0.07	0.06	0.06	0.07	0.06	0.06	0.06	0.05	0.06	0.06	0.05	0.06
MgO	1.79	1.84	1.74	1.63	1.64	1.59	1.53	1.58	1.39	1.44	1.43	1.20	1.30	1.27	1.13	1.25
CaO	5.46	5.51	5.27	5.40	5.29	5.40	5.04	5.18	5.05	5.23	4.62	4.66	4.55	4.48	4.16	4.48
Na_2O	3.85	3.72	3.83	3.91	3.77	3.82	3.79	4.08	4.19	3.99	3.76	3.95	3.86	3.95	3.70	3.93
K_2O	1.70	1.84	1.86	1.76	1.83	1.79	1.77	1.64	1.73	1.73	2.20	2.12	2.16	2.14	2.48	2.15
P_2O_5	0.23	0.24	0.22	0.21	0.22	0.22	0.20	0.21	0.19	0.20	0.20	0.18	0.18	0.18	0.16	0.18
S	<0.02	<0.02	<0.02	<0.02	<0.02	<0.02	<0.02	<0.02	<0.02	<0.02	<0.02	<0.02	<0.02	<0.02	<0.02	<0.02
H_2O+	0.95	0.87	0.90	0.80	0.85	0.69	0.95	0.76	0.79	0.74	0.79	0.75	0.92	0.62	0.77	0.64
H_2O-	0.21	0.11	0.11	.011	0.22	0.09	0.15	0.11	0.10	0.12	0.19	0.05	0.16	0.15	0.17	0.11
CO_2	0.10	0.10	0.21	0.09	0.05	0.05	0.12	0.10	0.27	0.17	0.34	0.10	0.08	0.15	0.18	0.08
rest	0.23	0.24	0.24	0.24	0.22	0.24	0.24	0.22	0.21	0.24	0.23	0.22	0.23	0.20	0.26	0.21
O=S																
Total	99.80	99.86	99.91	100.07	99.97	99.59	99.54	100.17	99.73	100.11	99.79	99.84	100.01	99.68	98.78	99.90
Ba	770	755	695	865	735	725	990	735	720	915	765	740	805	585	1050	715
Rb	56	60	63	53	63	58	53	49	49	46	84	69	80	68	92	78
Sr	585	574	600	595	580	616	540	575	580	615	523	560	560	503	503	550
Pb	8	9	8	9	9	12	8	9	11	9	13	9	12	10	13	12
Th	6.2	8.2	10.4	5.6	4.4	10.0	4.2	7.2	4.6	6.0	10.6	5.6	11.2	11.4	11.0	11.4
U	1.8	1.6	1.8	1.2	1.6	2.2	1.4	2.2	2.0	1.4	2.4	1.4	2.8	1.8	2.0	1.8
Zr	191	189	200	177	196	187	166	134	150	152	199	157	178	189	183	165
Nb	9.5	11.5	10.5	10.0	11.5	13.5	13.0	9.5	8.0	10.0	12.5	7.5	10.0	10.5	11.0	7.0
Y	13	15	15	13	14	17	25	13	14	13	17	10	13	16	14	7
La	23	25	33	19	18	25	14	21	11	19	23	18	21	27	23	31
Ce	49	55	74	43	42	59	38	45	31	46	58	38	47	62	56	59
Nd		22	28			25					23	13	18	23	21	
Sc	9	9	9	7	8	8	8	9	8	8	8	7	7	6	6	6
V	48	76	58	41	44	68	47	53	50	41	59	51	44	44	48	34
Cr	11	19	24	14	15	14	8	14	10	15	16	11	8	11	23	13
Mn	560	505	470	500	530	445	495	545	465	460	450	390	455	500	370	430
Ni	2	7	8	3	2	3	<1	1	<1	3	5	5	2	3	6	2
Cu	1	2	1	<1	2	1	<1	<1	<1	1	<1	1	3	2	1	<1
Zn	118	109	114	106	106	101	107	107	99	98	104	92	101	106	92	96
Ga	22.8	22.8	23.0	22.4	22.0	22.6	21.6	21.8	21.6	21.4	22.8	22.0	22.0	22.2	21.6	21.8

TABLE 1a. (continued)

	Unit I								Unit II						
	Tonalites and Granodiorites						Mafic Inclusions		Tonalites and Granodiorites						
	LTS301	LTS361	LTS363	LTS218	LTS298	LTS322	LTS216	LTS320	LTS148	LTS287	LTS329	LTS289	LTS368	LTS328	LTS326
SiO_2	66.56	67.67	68.07	69.44	69.56	70.06	48.89	55.42	62.66	63.79	64.18	64.90	65.01	65.35	65.58
TiO_2	0.66	0.61	0.56	0.49	0.46	0.49	1.98	1.24	0.95	0.85	0.83	0.88	0.81	0.73	0.82
Al_2O_3	16.28	15.44	15.72	14.93	15.28	15.22	19.46	16.10	17.11	15.87	17.10	15.98	16.53	16.28	16.31
Fe_2O_3	0.85	1.41	1.23	0.72	0.71	0.58	2.04	1.58	0.88	0.80	0.64	0.96	0.85	1.40	0.76
FeO	2.37	1.78	1.64	1.72	1.57	1.76	7.32	7.05	3.73	3.13	3.28	3.12	2.79	2.73	3.05
MnO	0.06	0.05	0.04	0.03	0.04	0.04	0.13	0.16	0.06	0.06	0.06	0.08	0.06	0.07	0.06
MgO	1.21	1.08	1.01	0.85	0.77	0.81	3.56	4.29	2.12	1.52	1.58	1.59	1.33	1.32	1.38
CaO	4.26	3.69	4.25	3.32	3.51	3.34	6.80	7.58	5.52	4.67	5.24	4.81	4.85	4.55	4.61
Na_2O	4.00	3.50	3.82	3.38	3.53	3.62	4.13	3.21	3.87	3.81	4.00	3.59	4.03	3.79	3.75
K_2O	2.17	2.84	1.56	3.25	3.01	3.06	2.91	1.65	1.62	1.98	1.55	2.17	1.92	2.09	2.26
P_2O_5	0.17	0.14	0.12	0.11	0.11	0.11	0.44	0.22	0.22	0.19	0.20	0.21	0.19	0.18	0.18
S	<0.02	<0.02	<0.02	<0.02	<0.02	<0.02	<0.02	0.02	<0.02	<0.02	<0.02	<0.02	<0.02	<0.02	<0.02
H_2O+	0.68	0.84	0.87	0.63	0.46	0.51	1.38	1.16	0.71	1.03	0.82	0.93	0.79	0.87	0.75
H_2O-	0.07	0.19	0.16	0.13	0.16	0.07	0.17	0.11	0.03	0.14	0.13	0.13	0.15	0.21	0.14
CO_2	0.13	0.13	0.10	0.33	0.15	0.12	0.12	0.15	0.09	0.32	0.18	0.14	0.06	0.10	0.15
rest	0.19	0.24	0.20	0.31	0.31	0.22	0.33	0.25	0.25	0.23	0.22	0.24	0.23	0.20	0.24
O=S															
Total	99.66	99.61	99.35	99.64	99.63	100.01	99.66	100.18	99.82	98.39	100.01	99.73	99.60	99.87	100.04
Ba	515	1070	730	1640	1685	970	1095	745	930	750	760	830	785	695	940
Rb	78	94	48.5	89	74	91	111	45	49	72	48	71	62	79	89
Sr	505	493	550	513	521	426	582	491	622	502	600	517	570	468	525
Pb	12	14	8	15	11	15	9	6	6	11	8	11	10	11	13
Th	13.8	17.0	8.2	10.6	9.0	10.8	3.0	0.2	5.4	11.8	6.0	11.4	8.0	9.2	11.4
U	2.4	1.6	1.4	1.6	1.6	1.8	1.0	<0.2	0.8	2.8	1.2	2.4	2.6	2.0	3.6
Zr	178	149	137	146	122	138	339	150	178	180	174	180	185	174	180
Nb	10.0	7.5	5.0	8.0	7.5	9.0	17.0	9.5	12.5	14.0	8.0	13.0	11.0	10.5	10.5
Y	12	8	4	8	7	13	26	24	16	19	10	22	16	18	17
La	23	17	25	23	20	19	16	12	15	28	22	29	20	24	27
Ce	49	35	55	48	41	40	40	41	38	62	43	63	48	50	59
Nd	17			14	11	11	26		18	25		26			
Sc	6	4	3	4	5	5	21	20	9	8	8	8	7	8	6
V	42	33	29	35	26	21	148	125	64	62	43	52	41	33	33
Cr	14	13	10	14	12	8	8	110	16	19	13	19	7	11	9
Mn	480	380	300	265	290	335	1015	1215	450	490	495	590	455	565	460
Ni	4	<1	<1	4	2	<1	8	11	6	6	2	6	<1	2	1
Cu	3	<1	5	1	9	<1	32	2	3	2	<1	2	<1	<1	<1
Zn	94	91	76	68	60	62	213	202	110	107	108	102	100	100	98
Ga	21.8	20.0	19.4	18.8	18.2	18.4	28.6	22.8	23.4	22.0	22.0	21.2	21.8	20.6	20.8

TABLE 1a. (continued)

	Unit II			Unit III										
	Tonalites and Granodiorites			Tonalites and Granodiorites										
	LTS149	LTS327	LTS288	LTS376	LTS360	LTS290	LTS374	LTS369	LTS152	LTS335	LTS331	LTS151	LTS146	LTS373
SiO_2	65.74	66.79	70.46	63.47	63.60	64.50	64.68	64.99	66.08	66.53	66.67	66.72	66.79	66.83
TiO_2	0.72	0.66	0.41	0.81	0.80	0.77	0.77	0.73	0.69	0.62	0.63	0.63	0.59	0.53
Al_2O_3	16.58	15.83	14.82	16.97	16.95	16.96	16.74	16.45	16.73	16.59	16.55	16.68	16.77	16.51
Fe_2O_3	0.64	0.54	0.70	0.71	0.81	0.85	0.65	0.94	0.48	0.90	0.60	0.56	0.74	0.32
FeO	2.87	3.17	1.18	3.17	3.27	2.88	3.06	2.76	2.75	2.27	2.56	2.62	2.41	2.47
MnO	0.05	0.07	0.03	0.06	0.06	0.07	0.06	0.06	0.05	0.05	0.06	0.05	0.05	0.05
MgO	1.29	1.16	0.69	1.48	1.44	1.44	1.43	1.42	1.24	1.13	1.13	1.12	1.07	0.97
CaO	4.48	4.01	3.05	5.00	4.89	4.82	4.84	4.18	4.31	4.35	4.19	4.37	4.17	4.20
Na_2O	3.91	3.86	3.23	4.00	3.96	4.03	3.98	3.81	4.12	4.04	3.99	4.23	4.07	4.04
K_2O	2.41	2.65	3.89	2.11	2.13	2.04	2.01	2.21	2.06	2.11	2.30	1.88	2.23	1.89
P_2O_2	0.18	0.16	0.09	0.20	0.20	0.19	0.20	0.20	0.17	0.16	0.17	0.16	0.16	0.15
S	<0.02	<0.02	<0.02	<0.02	<0.02	<0.02	<0.02	<0.02	<0.02	<0.02	<0.02	<0.02	<0.02	<0.02
H_2O+	0.60	0.65	0.53	0.77	0.81	0.89	0.75	1.16	0.61	0.68	0.63	0.66	0.70	0.69
H_2O-	0.08	0.08	0.21	0.13	0.09	0.11	0.10	0.37	0.06	0.12	0.10	0.04	0.05	0.08
CO_2	0.15	0.15	0.13	0.14	0.09	0.19	0.07	0.12	0.10	0.07	0.11	0.08	0.08	0.14
rest	0.22	0.21	0.37	0.21	0.22	0.22	0.19	0.21	0.23	0.24	0.23	0.19	0.25	0.21
O=S														
Total	99.92	99.99	99.79	99.23	99.32	99.96	99.53	99.61	99.68	99.86	99.92	99.99	100.13	99.08
Ba	815	845	2235	605	705	700	505	710	855	930	880	500	1025	665
Rb	83	83	95	78	76	82	84	90	72	64	67	72	67	77
Sr	452	405	505	565	575	579	520	500	558	570	545	547	550	565
Pb	10	14	19	11	12	12	12	11	10	11	11	8	9	12
Th	9.8	8.4	9.4	9.2	7.2	10.6	11.0	7.8	9.2	7.2	5.6	9.6	8.8	8.6
U	2.4	2.2	1.6	2.8	2.8	2.4	2.6	2.4	2.2	1.6	1.2	1.8	1.8	2.0
Zr	186	179	107	195	186	180	184	176	162	168	165	170	165	186
Nb	10.0	9.5	8.5	10.0	12.0	10.0	9.5	8.5	8.5	8.5	9.0	9.0	9.0	8.5
Y	19	26	10	11	21	11	14	12	9	13	13	14	14	12
La	22	16	20	20	13	23	25	19	19	21	21	22	20	19
Ce	50	43	46	38	31	49	52	36	41	43	45	48	46	43
Nd	20		13			17			14			18	16	
Sc	6	7	4	8	8	7	7	7	6	6	6	6	5	6
V	45	30	33	46	48	51	45	42	48	28	29	42	36	22
Cr	16	10	9	10	10	13	9	9	17	12	12	10	10	8
Mn	420	580	250	500	500	540	480	480	405	420	430	380	355	385
Ni	5	<1	3	<1	<1	3	<1	<1	4	<1	1	4	3	1
Cu	2	1	<1	3	<1	2	1	2	<1	<1	<1	<1	1	<1
Zn	85	85	55	100	102	97	90	93	93	91	93	87	87	95
Ga	21.2	19.4	17.4	23.2	23.6	23.0	22.0	22.0	22.2	21.4	21.6	22.0	21.8	21.8

TABLE 1b. Major Tonalites

	Unit III															
	Tonalites and Granodiorites															
	LTS370	LTS222	LTS371	LTS337	LTS336	LTS334	LTS333	LTS359	LTS375	LTS332	LTS366	LTS367	LTS145	LTS292	LTS365	LTS212
SiO_2	66.91	66.92	66.96	67.02	67.06	67.07	67.14	67.17	67.24	67.63	67.68	67.79	67.90	69.16	69.83	70.11
TiO_2	0.57	0.62	0.61	0.68	0.56	0.59	0.67	0.60	0.53	0.58	0.52	0.56	0.56	0.44	0.40	0.45
Al_2O_3	16.37	16.26	15.99	16.46	16.52	16.22	16.08	16.15	16.13	16.17	15.99	15.63	15.41	15.51	14.95	15.02
Fe_2O_3	0.85	1.32	0.60	0.59	0.50	0.58	0.69	0.55	0.58	0.64	0.70	0.64	0.68	0.70	0.54	0.57
FeO	2.16	1.97	2.41	2.49	2.41	2.81	2.66	2.58	2.38	2.26	2.16	2.36	2.23	1.84	1.81	1.91
MnO	0.05	0.05	0.05	0.06	0.05	0.05	0.06	0.05	0.05	0.05	0.06	0.05	0.05	0.04	0.04	0.04
MgO	1.01	1.11	1.12	1.10	1.06	1.19	1.22	1.10	1.03	1.04	0.89	0.98	1.94	0.78	0.69	0.76
CaO	3.96	4.26	4.20	4.29	4.28	4.12	4.15	4.13	4.18	3.92	3.54	3.80	3.75	3.20	2.98	3.08
Na_2O	4.06	4.17	3.98	4.02	4.01	3.89	3.87	3.95	3.89	3.90	4.01	4.03	3.83	3.78	3.70	3.71
K_2O	2.48	1.75	2.22	2.10	1.95	2.16	2.24	1.82	2.13	2.57	2.90	2.29	2.44	3.05	3.04	2.86
P_2O_5	0.15	0.17	0.15	0.16	0.16	0.17	0.16	0.15	0.13	0.14	0.13	0.15	0.13	0.11	0.10	0.11
S	<0.02	<0.02	<0.02	<0.02	<0.02	<0.02	<0.02	<0.02	<0.02	<0.02	<0.02	<0.02	<0.02	<0.02	<0.02	<0.02
H_2O+	0.77	0.76	0.66	0.63	0.68	0.69	0.62	0.74	0.67	0.65	0.64	0.76	0.74	0.76	0.64	0.64
H_2O-	0.11	0.18	0.08	0.08	0.12	0.11	0.09	0.10	0.13	0.06	0.09	0.16	0.04	0.09	0.08	0.10
CO_2	0.11	0.22	0.13	0.03	0.17	0.15	0.07	0.11	0.10	0.11	0.09	0.05	0.17	0.19	0.14	0.12
rest	0.25	0.19	0.25	0.23	0.22	0.24	0.25	0.20	0.18	0.24	0.24	0.22	0.25	0.27	0.24	0.27
O=S																
Total	99.81	99.95	99.41	99.94	99.75	100.04	99.97	99.40	99.35	99.96	99.64	99.47	100.12	99.92	99.18	99.75
Ba	1090	435	1060	945	845	995	1060	680	600	1040	1010	805	1130	1325	1130	1280
Rb	76	76	64	66	66	68	69	62	80	85	98	73	69	79	79	82
Sr	550	537	540	555	595	545	535	550	488	510	469	487	520	505	443	479
Pb	13	10	11	11	12	10	11	10	14	15	14	11	10	13	13	13
Th	8.6	11.2	8.8	6.6	6.0	8.4	7.0	6.8	11.0	8.2	11.0	8.8	9.0	10.8	11.0	14.0
U	2.0	1.6	1.6	2.4	1.4	1.2	1.6	1.6	2.0	1.8	2.0	1.4	1.4	1.4	1.4	1.4
Zr	174	174	171	159	158	161	175	158	129	154	172	191	151	178	169	172
Nb	9.0	9.5	9.5	11.5	6.5	7.0	10.0	10.0	7.0	9.0	9.0	10.5	7.5	7.5	7.5	8.5
Y	11	12	15	23	8	6	15	12	7	12	11	16	12	8	7	8
La	22	23	22	16	15	28	20	20	18	19	24	24	20	22	25	26
Ce	46	52	50	40	32	54	44	42	39	42	53	52	45	48	57	57
Nd		18											15	15		18
Sc	5	5	5	6	6	6	6	5	6	5	5	5	6	4	4	4
V	30	45	34	28	26	30	31	32	32	27	26	30	38	22	17	31
Cr	7	13	11	11	10	12	12	9	9	9	5	9	12	9	11	15
Mn	395	375	405	435	375	425	440	375	405	400	430	415	370	340	335	300
Ni	<1	3	<1	1	<1	<1	1	<1	<1	<1	<1	<1	4	2	<1	5
Cu	<1	<1	<1	<1	<1	<1	<1	<1	<1	<1	3	<1	1	<1	<1	<1
Zn	92	97	89	91	90	95	95	97	76	84	86	95	82	83	79	78
Ga	21.2	22.8	20.4	20.8	20.4	20.8	20.8	22.2	19.8	20.8	20.8	20.6	20.2	19.8	19.2	19.8

TABLE 1b. (continued)

	Unit III								
	Granodiorite	Altered		Mafic Inclusions				Dyke Rocks	
	LTS358	LTS213	LTS297	LTS379	LTS291	LTS377	LTS378	LTS214	LTS221
SiO_2	70.57	67.65	68.65	57.02	58.70	59.77	60.79	58.36	62.91
TiO_2	0.40	0.53	0.51	1.45	1.41	1.26	1.18	1.31	0.86
Al_2O_3	14.79	16.45	15.70	16.55	17.18	17.38	17.01	18.29	16.17
Fe_2O_3	0.44	0.50	0.64	1.66	1.95	1.06	1.38	1.70	1.37
FeO	1.50	2.31	2.22	5.53	3.79	4.21	3.87	3.96	3.45
MnO	0.03	0.04	0.05	0.14	0.12	0.09	0.08	0.06	0.07
MgO	0.71	0.94	0.81	3.13	2.21	2.16	2.24	1.80	2.05
CaO	2.98	4.11	3.65	6.80	6.82	6.19	5.87	6.41	5.40
Na_2O	3.15	4.14	3.79	3.76	4.08	4.03	3.77	3.99	3.48
K_2O	3.64	1.80	2.36	1.69	1.45	1.71	1.79	1.65	1.97
P_2O_5	0.09	0.15	0.13	0.31	0.37	0.31	0.27	0.35	0.16
S	<0.02	<0.02	<0.02	<0.02	<0.02	0.02	<0.02	<0.02	<0.02
H_2O+	0.63	0.68	0.64	1.12	0.98	1.01	1.08	0.93	0.96
H_2O-	0.13	0.08	0.12	0.11	0.19	0.14	0.20	0.26	0.24
CO_2	0.12	0.18	0.23	0.05	0.12	0.07	0.02	0.15	0.16
rest	0.31	0.21	0.23	0.20	0.21	0.26	0.26	0.33	0.19
O=S						0.01			
Total	99.49	99.77	99.73	99.52	99.58	99.66	99.81	99.55	99.44
Ba	1810	630	820	390	375	795	825	1095	570
Rb	80	86	96	78	64	65	69	44.5	80
Sr	520	556	480	482	590	670	650	790	432
Pb	14	14	16	9	11	8	7	7	12
Th	7.0	12.0	16.0	1.0	3.4	4.2	3.8	7.2	17.2
U	1.0	4.8	4.2	2.2	0.8	1.6	1.2	0.4	4.8
Zr	122	183	243	223	277	250	240	390	124
Nb	7.0	10.0	9.5	11.5	14.0	11.5	9.5	14.5	9.0
Y	6	10	10	19	22	16	14	18	13
La	17	24	30	17	11	21	26	33	23
Ce	33	55	69	31	32	49	51	77	44
Nd		19	22		21			31	14
Sc	3	5	4	12	13	10	9	8	8
V	19	33	19	108	69	65	68	61	83
Cr	9	14	11	46	29	18	20	11	12
Mn	235	305	375	1060	915	665	605	495	580
Ni	<1	3	1	6	7	1	2	6	6
Cu	<1	<1	<1	15	14	12	10	1	<1
Zn	46	91	74	174	136	128	128	159	97
Ga	16.6	22.4	20.2	22.8	23.8	23.8	23.2	26.8	20.8

TABLE 2. Early Intrusives

	TONALITE OF SNOW CREEK		GRANODIORITE OF POPPET CREEK		ISOLATED SMALL MASSES					GRANITE OF PENROD CANYON	
	LTS302	LTS035	LTS317	LTS114	LTS381	LTS316	LTS211	LTS315	LTS382	LTS364	LTS318
SiO_2	63.21	63.98	63.77	67.42	62.59	63.04	68.91	69.61	73.12	71.92	73.70
TiO_2	0.96	0.97	0.75	0.52	0.85	0.82	0.44	0.40	0.24	0.19	0.09
Al_2O_3	16.68	17.02	15.81	15.05	17.43	17.65	15.12	15.07	13.52	14.94	14.61
Fe_2O_3	1.58	0.84	0.81	0.87	0.49	0.73	0.76	0.54	0.56	0.39	0.23
FeO	2.67	3.66	4.07	2.80	3.60	3.56	1.59	2.44	1.61	1.36	0.86
MnO	0.07	0.06	0.08	0.07	0.06	0.07	0.03	0.06	0.04	0.05	0.03
MgO	1.61	1.66	2.39	1.60	1.65	1.60	0.71	0.87	0.37	0.35	0.16
CaO	5.14	5.27	5.17	3.71	5.58	5.72	3.50	3.05	1.90	1.66	1.23
Na_2O	3.74	3.81	3.07	3.09	3.98	3.81	3.96	3.44	3.26	4.16	3.99
K_2O	1.95	1.84	2.53	3.62	1.50	1.56	1.78	3.52	4.12	3.42	4.25
P_2O_5	0.21	0.24	0.12	0.09	0.21	0.21	0.11	0.07	0.05	0.05	0.04
S	<0.02	<0.02	<0.02	<0.02	<0.02	<0.02	<0.02	<0.02	0.02	<0.02	<0.02
H_2O+	1.26	0.70	0.89	0.72	0.89	0.75	0.62	0.58	0.49	0.54	0.28
H_2O-	0.25	0.04	0.16	0.14	0.09	0.09	0.21	0.12	0.12	0.08	0.09
CO_2	0.20	0.01	0.13	0.18	0.20	0.11	0.06	0.14	0.19	0.15	0.09
rest	0.27	0.24	0.20	0.20	0.21	0.20	0.21	0.20	0.17	0.15	0.11
O=S									0.01		
Total	99.80	100.34	99.95	100.08	99.33	99.92	98.01	100.11	99.77	99.41	99.76
Ba	940	830	775	805	690	680	660	940	885	720	445
Rb	61	50	98	137	46.5	51	71	113	92	130	165
Sr	630	603	284	232	627	545	535	227	142	145	79
Pb	11	11	11	18	7	9	10	13	11	22	25
Th	11.6	6.6	12.2	19.4	2.4	3.2	12.6	15.6	12.6	8.2	6.8
U	2.4	1.6	2.0	2.2	0.6	1.2	3.4	1.4	1.2	2.4	1.6
Zr	186	162	169	166	158	149	218	143	141	107	71
Nb	13.5	11.0	9.0	10.0	9.0	7.5	9.0	8.0	8.0	12.0	11.5
Y	28	20	25	20	12	11	11	13	13	12	13
La	33	25	21		11	10	29	29	19	13	11
Ce	82	58	51	61	26	25	65	56	52	26	22
Nd	38	24		19			22				
Sc	8	8	14	9	9	7	4	6	5	4	3
V	55	57	76	56	54	41	28	27	10	3	<1
Cr	12	10	34	26	12	9	11	11	7	6	5
Mn	520	455	640	560	495	545	255	465	340	390	255
Ni	4	4	6	5	<1	1	4	<1	<1	<1	<1
Cu	2	2	5	2	<1	3	<1	<1	<1	2	<1
Zn	109	93	78	72	107	102	69	61	43	66	57
Ga	22.0	21.4	17.6	17.4	22.0	22.0	21.6	16.6	15.8	17.4	18.0

TABLE 3. Small Intrusions From Around Tahquitz Peak

	RELATIVELY UNCONTAMINATED		CONTAMINATED					DIFFERENTIATES	
	LTS314	LTS293	LTS271	LTS380	LTS383	LTS384	LTS311	LTS294	LTS295
SiO_2	65.86	66.70	65.95	67.89	68.20	68.83	68.91	59.91	78.53
TiO_2	0.71	0.61	0.39	0.41	0.34	0.30	0.44	0.84	0.10
Al_2O_3	16.20	16.04	17.24	15.47	16.34	15.93	16.32	16.48	11.84
Fe_2O_3	0.73	0.59	0.60	0.63	0.96	0.61	0.35	1.07	0.18
FeO	3.28	3.33	3.59	3.43	3.06	2.97	2.66	5.99	0.56
MnO	0.07	0.08	0.03	0.09	0.17	0.14	0.05	1.80	0.02
MgO	1.27	1.21	0.29	0.39	0.29	0.21	0.55	1.80	0.14
CaO	4.43	3.54	3.57	3.35	3.05	3.02	3.44	3.92	1.64
Na_2O	3.82	4.35	4.66	4.42	4.50	4.30	4.87	3.77	3.07
K_2O	2.18	2.01	2.00	2.02	1.72	2.30	1.39	4.14	3.28
P_2O_5	0.17	0.12	1.08	0.11	0.05	0.06	0.04	0.20	0.03
S	<0.02	<0.02	<0.02	<0.02	<0.02	<0.02	<0.02	<0.02	<0.02
H_2O+	0.75	0.75	0.60	0.60	0.49	0.51	0.49	0.93	0.30
H_2O-	0.10	0.09	0.11	0.10	0.06	0.11	0.12	0.10	0.06
CO_2	0.19	0.16	0.10	0.06	0.08	0.18	0.18	0.21	0.06
rest	0.21	0.15	0.46	0.49	0.29	0.42	0.22	0.28	0.15
O=S									
	99.97	99.73	99.67	99.47	99.60	99.89	100.03	99.82	99.96
Ba	720	410	2490	3140	1290	2550	785	1200	855
Rb	81	108	76	39	56	63	52	151	83
Sr	465	267	321	314	259	282	288	249	193
Pb	11	11		8	15	9	9	16	16
Th	7.0	13.2	7.2	6.4	10.0	4.6	6.6	9.4	7.2
U	1.8	1.8	2.2	1.8	3.4	2.0	1.0	1.2	1.2
Zr	186	126	489	439	444	377	366	224	61
Nb	10.5	11.5	19.0	11.0	13.5	15.0	12.0	19.0	5.5
Y	16	12	21	22	54	30	9	60	8
La	18	21	71	44	49	54	39	17	8
Ce	34	46	163	92	105	119	80	48	18
Nd		15	58					24	6
Sc	8	5	34	11	15	18	14	17	1
V	33	45	17	7	1	<1	4	69	5
Cr	11	11	13	9	9	12	11	16	7
Mn	545	625	235	680	1340	1050	365	1360	125
Ni	1	4	5	<1	<1	<1	<1	4	<1
Cu	1	1	1	2	<1	<1	<1	1	5
Zn	98	103	123	95	69	92	109	164	18
Ga	20.8	21.0	23.6	20.2	21.0	19.8	23.4	23.8	17.8

units varies from about 62.5 to 70.6 wt %. Relationships between major elements are remarkably systematic. Figure 2 shows Harker diagrams for selected major elements. TiO_2, Al_2O_3, Fe_2O_3, FeO, MnO, MgO, CaO and P_2O_5 all decrease linearly with increasing SiO_2. The trend for MgO, however, shows a slight break in slope at about 66-67 wt % SiO_2. Na_2O increases slightly with increasing SiO_2, then falls rapidly in the few most felsic rocks. K_2O shows considerable scatter, but with an approximate trend to increasing K_2O as SiO_2 increases.

Although all three units overlap in chemical composition (but see below), samples from unit III are slightly more felsic and more homogeneous than are samples from the other two units. Nearly 60% of analyses of rocks from this unit (and a comparable or larger area of outcrop) show an extremely restricted range in SiO_2 of 66.5-68.0 wt %. Only a relatively small proportion of the rocks sampled from the other two units (30%) have more than 66.5% SiO_2, consistent with field observations that they are generally a little more mafic than unit III. Units I and II also show restricted compositional ranges, with >60% of samples having between 63 and 66% SiO_2.

In general, the three units show a near complete overlap in the ranges of their chemical compositions. There are, however, a few exceptions. Rocks from unit III generally have less TiO_2 and more Al_2O_3 and Na_2O for a given SiO_2 content than do rocks from units I and II (Figure 2); rocks from unit III also show a much wider variation in K_2O content at a given SiO_2 than do rocks from the other two units.

H_2O^+ correlates negatively with SiO_2, as would be predicted from the decreasing abundance of hydrous phases as the rocks become more felsic. Values fall from around 1.0 wt % in the most mafic rocks to 0.5-0.6 wt % in the most felsic. Burnham [1979] estimates that a minimum of 3.0 wt % H_2O in the liquid is needed before amphibole

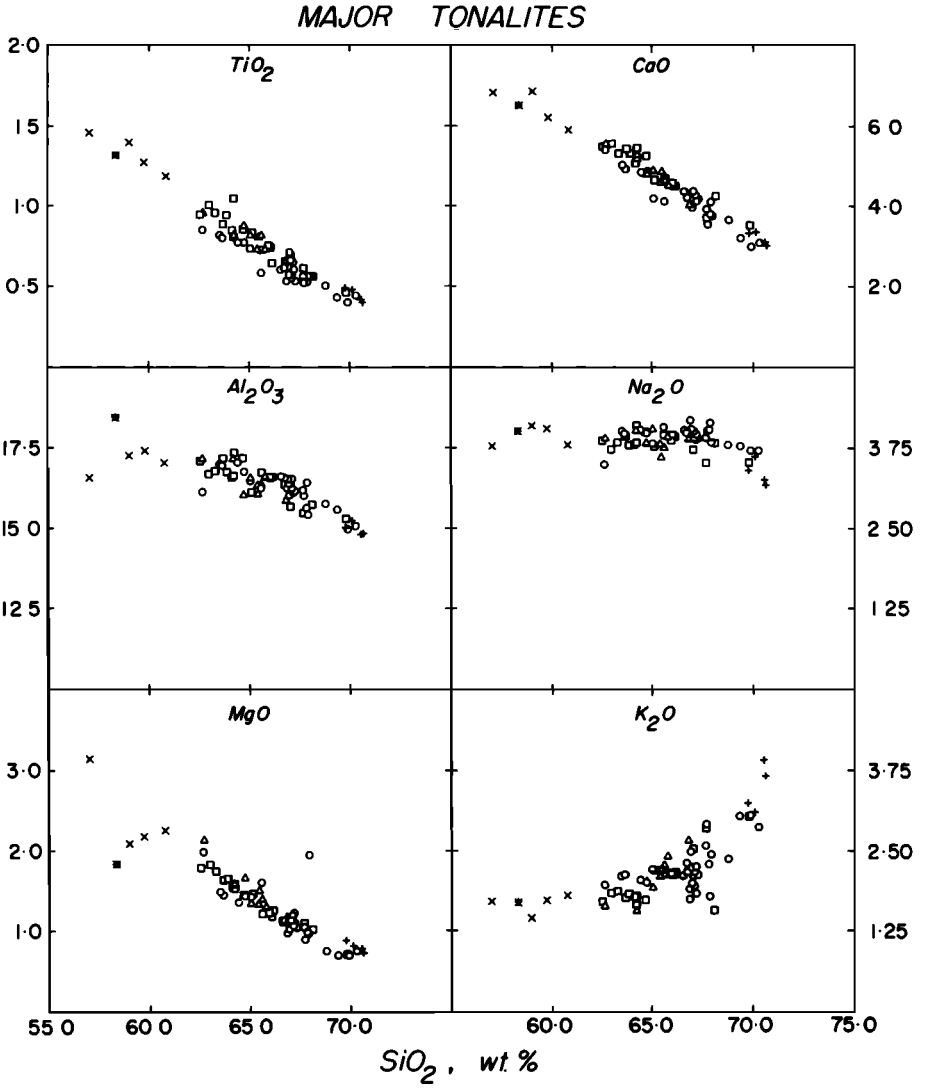

Fig. 2. Harker diagrams for selected major elements. Squares, unit I; triangles, unit II; circles, unit III; crosses, inclusions; asterisks, dyke rocks; pluses, felsic differentiates.

will crystallize; as amphibole is a stable phase in all of these rocks, it is implied that a considerable amount of water has been lost from the system during crystallization.

Trace elements. Trace element correlations with SiO_2 show much more complex variation patterns than do the more abundant components (Figures 3-5). Ba, Rb, Pb, and Th show a general tendency to increase with SiO_2, Sr and Zr decrease slightly, whereas Sc, V, Cr, Zn, and Ga show a pronounced linear decrease with increasing SiO_2. U, Nb, Y, La, Ce, Nd, Ni, and Cu show no systematic variation with changing SiO_2 content. These variations are similar to those observed in many other continental margin and island arc suites [e.g., Bateman and Chappell, 1979; Gill, 1981].

Felsic "differentiates". Four samples were collected that are considerably more felsic than the typical surrounding rock. They are biotite-poor (5-10%) and K-feldspar-rich (8-15%) relative to the common tonalites. Three of these samples (218, 288, 358) are from areas where schlieren are prominently developed, and field relations suggest that they are the products of crystal-liquid separation (perhaps by flow differentiation) at a relatively small scale (tens to hundreds of meters). The fourth sample (322) is from a large mass of felsic rock (perhaps, 50x1000 m) near the center of unit I. Although representative of the rock at the local scale (hundreds to a thousand meters), this sample is considerably more felsic than the bulk of this unit. Again, it appeared that crystal fractionation might be a viable mechanism for generating these centrally located more felsic rocks [cf. Bateman and Chappell, 1979], and this sample was collected in part to test this hypothesis.

These four samples are distinguished on the various element-element diagrams. In the field there is an apparent complete gradation between these most felsic end-member compositions and the more typical tonalites. Relatively felsic rocks are overrepresented in the analyses in terms of relative abundances (although the central region of unit III is relatively felsic), and this is reflected in an apparent high-SiO_2 group on the Harker diagrams.

The geochemical effects of these high-level processes are best seen in the behavior of K and

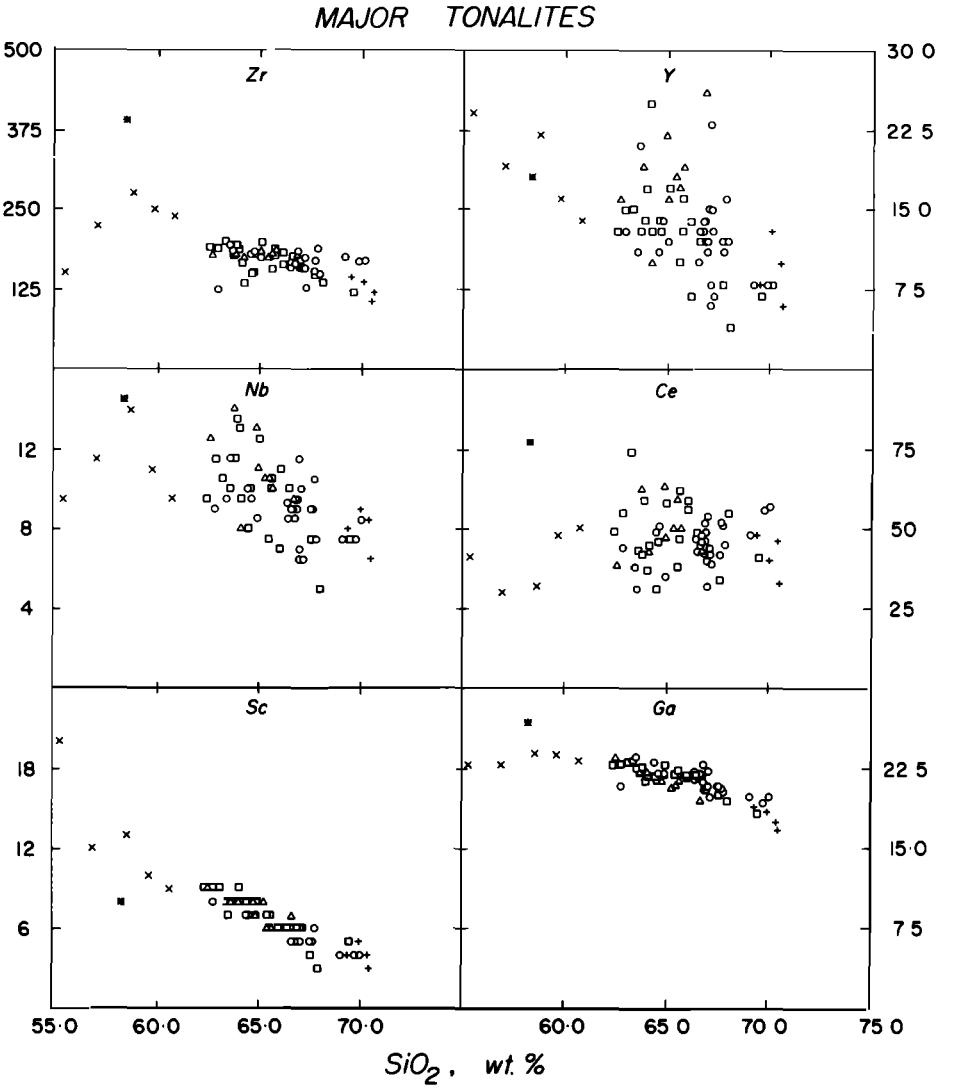

Fig. 3. Harker diagrams for Zr, Nb, Sc, Y, Ce, and Ga. Symbols as for Figure 2.

related elements (Rb and Ba). The four samples have, as expected from their mineralogy, high SiO_2 and K_2O. They also have high Ba (Ba increases linearly with K), and K/Rb increases dramatically in the more K-rich rocks. This is the expected behavior where biotite is an important crystallizing phase, as it is in these plutons. The linear covariation of K and Ba, with Ba increasing about 3 times more rapidly than K, argues that Ba is being relatively efficiently excluded from the minerals of the more mafic rocks (relative to K) and implies $D^{Ba}_{Biotite/liq} < 2$. This behavior is consistent with precipitation of the assemblage plagioclase + hornblende + biotite + quartz + titanite leaving a liquid enriched in SiO_2 and Ba and, to a lesser extent, K.

The geochemistry of these four samples is thus consistent with them having crystallized from evolved liquids formed by removal of the observed mineral phases from a less evolved earlier liquid; that is, they are the end products of fractional crystallization processes acting within the solidifying magma chamber. They thus potentially allow recognition of the effects of this process in less extreme cases.

Mafic Inclusions and Dyke Rocks

Field relations were interpreted by Hill [this issue] as showing that the common mafic inclusions were derived from mafic dykes that were emplaced into the solidifying magma chamber, and that both dyke rocks and mafic inclusions represent samples of liquid (plus suspended crystals) added to the inflating magma chambers. The field relations thus imply consanguineity of dyke rocks, mafic inclusions, and tonalites. However, the dyke rocks and mafic inclusions sample liquids, whereas the tonalites are precipitates fractionated from these liquids. The lack of felsic, differentiated rocks and the close similarity between tonalite compositions and any estimate for the bulk composition of each pluton suggest that the tonalites do closely approximate liquid compositions, perhaps with a small amount (≈1%) of felsic liquid removed.

Five mafic inclusions and a single mafic dyke rock have geochemical characteristics colinear with those of their host tonalites but are more mafic, spanning the SiO_2 range 55.4-60.8 wt % (cf. mafic tonalites 62.5-65.5). A sample of

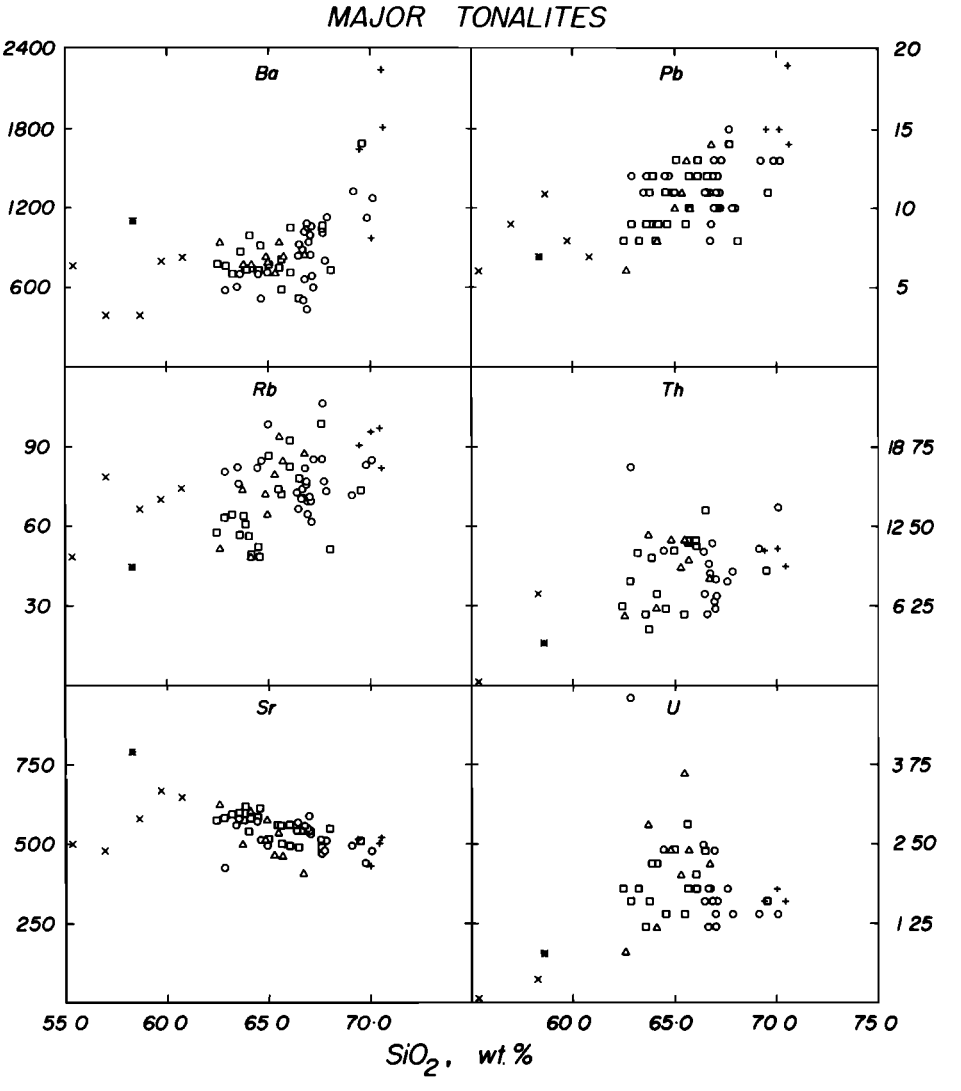

Fig. 4. Harker diagrams for Ba, Rb, Sr, Pb, Th, and U. Symbols as for Figure 2.

tonalitic dyke rock has SiO_2 = 62.9 wt %, and an overall composition that closely matches that of the mafic tonalites, further strengthening the inference that the tonalites closely approximate liquid compositions. The inclusion and dyke rock samples have geochemical characteristics that also strongly imply consanguineity, and they may represent samples of liquids containing various amounts of suspended crystals (particularly plagioclase and hornblende) that were chilled upon introduction into the crystallizing magma chamber. In particular, both analyzed dyke rocks contain abundant aligned plagioclase tablets, and the mafic dyke rock (214) is unusually plagioclase-rich (67 vol % plag). The chemical data for this sample (high Al_2O_3 and Sr) reflect this plagioclase enrichment.

A sixth mafic inclusion (216; not shown on the variation diagrams) is interpreted as a cognate inclusion; it appears to be part of a schliere reincorporated into the tonalite magma. With these exceptions, the mafic inclusion and dyke rock analyses cluster around the projection toward low SiO_2 defined by the trends of the tonalites. Thus either the compositions of the tonalites mimic those of liquids from which they solidified or the precipitation of more mafic minerals from a liquid to give a solid tonalite mirrors the fractionation trends of the evolving liquids (at least for the major elements), so that the composition of a particular tonalite approximates that of a liquid somewhat less evolved than the one from which it precipitated. The coherence of mineral chemical data between inclusions and tonalites [Hill, this issue] and their similar bulk Ca/(Ca + Na) and Mg/(Mg + Fe) would seem, at first glance, to preclude derivation of the tonalites from liquids having the compositions of either the inclusions or the tonalite dyke rock. However, a close chemical correspondence between added liquid and derived rocks is a feature (under certain conditions) of the intermittently recharged, continuously solidified magma chamber model developed below.

Insufficient data are available to test rigorously the extent of chemical interaction between inclusions and host rock. Several features of inclusions and dyke rocks (maintenance of distinct mineral compositions, maintenance of Sr isotope heterogeneity in some samples, general

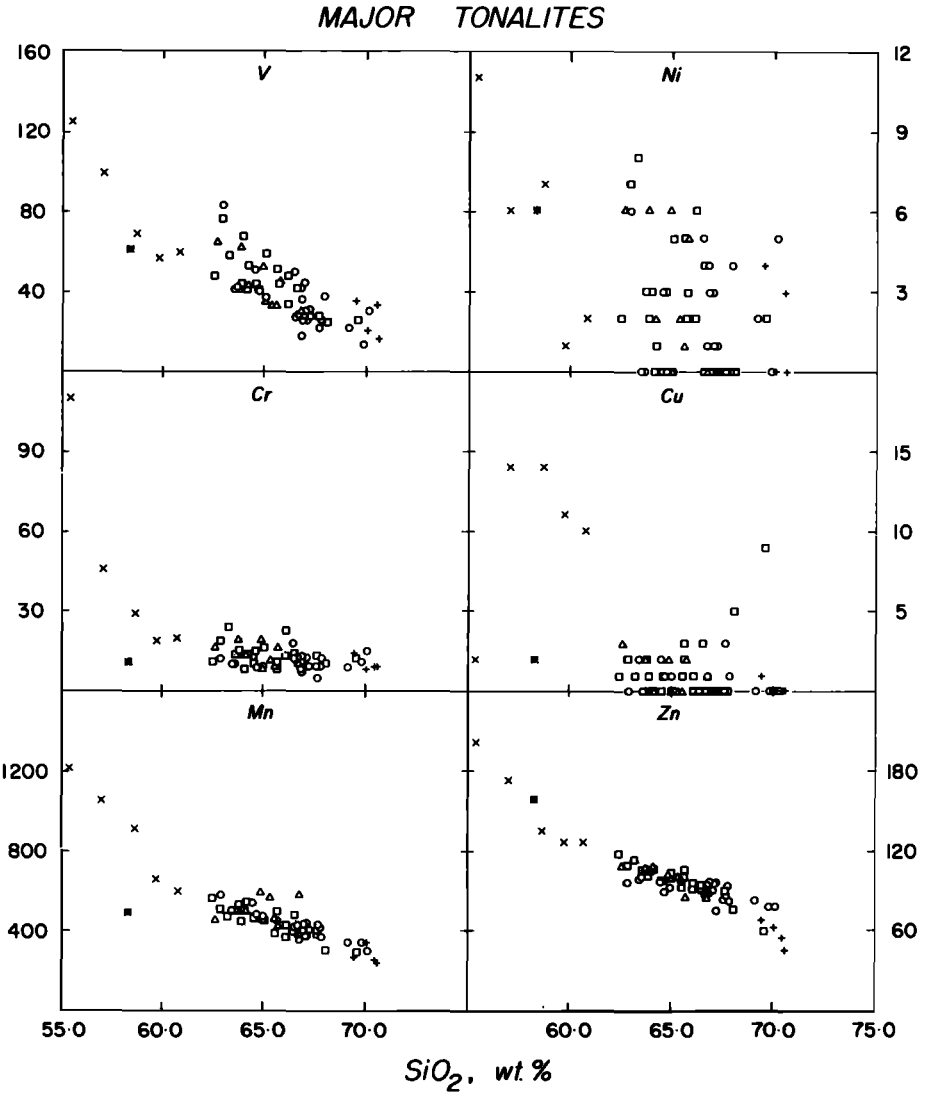

Fig. 5. Harker diagrams for V, Cr, Mn, Ni, Cu, and Zn. Symbols as for Figure 2.

absence of K-feldspar) imply limited, if any, chemical exchange with host liquids. The general geochemical similarity (of inclusion and host), and the large size of inclusions (to 1 m or more) and dykes (to 10 m) would also act to limit the rate and importance of exchange.

Mafic Tonalites

The more mafic tonalites show regular covariation of even the most incompatible elements; felsic tonalites and granodiorite, and particularly the felsic differentiates commonly do not. To illustrate this feature of these rocks, "mafic tonalites" are differentiated on Figures 6 and 7, plots of K-Rb, K-U, and Ca-Sr. The subdivision (SiO_2 < 65.5% for mafic tonalites) is an arbitrary subdivision of a continuum; nevertheless, it serves to illustrate graphically the point that the more mafic rocks have simpler geochemical interrelationships than do their more felsic counterparts. The felsic differentiates have geochemical characteristics most removed from those of the mafic tonalites; felsic tonalites and K-feldspar-poor granodiorites have intermediate characteristics (Figures 6 and 7). The mafic tonalites appear to approximate the compositions of new liquids added to the magma chambers. Mixtures of these new liquids (and suspended crystals) with fractionated magmas already within the chambers give rise to "hybrid" magmas from which the more SiO_2-rich rocks solidify. Direct evidence (the analyses of inclusions and dyke rocks) shows that the liquids being added to the chamber spanned at least the SiO_2 range 55-63 wt %; the trend of the mafic tonalites suggests that this range extends to at least 66 wt %. The relatively felsic bulk composition of the three major plutons (approximately 65-66 wt % SiO_2) implies that even more felsic liquids were being added. This is consistent with the range observed for the early intrusives (olivine gabbro to granite, although dominated by tonalite), which indicates that silicate liquids with a wide compositional range were moving upward through the crust immediately prior to formation (and probably during growth) of the large tonalite magma chambers.

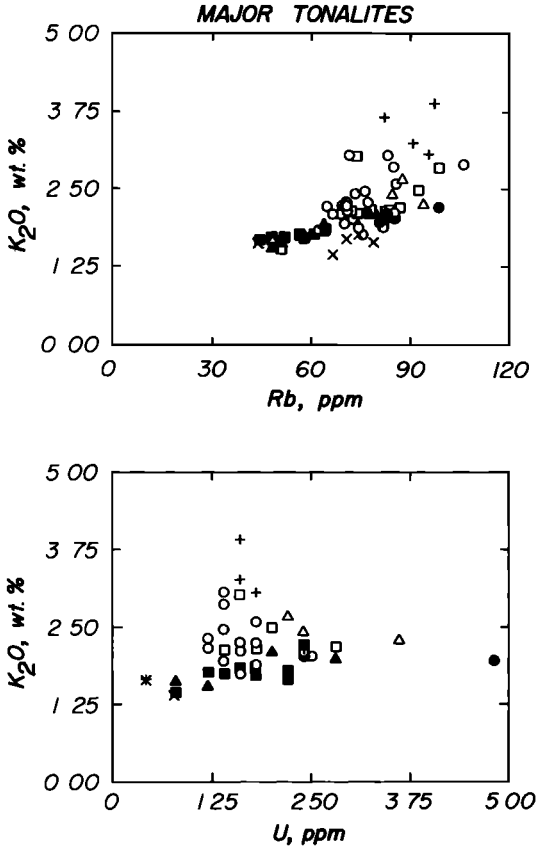

Fig. 6. Rb versus K_2O and U versus K_2O. Symbols as for Figure 2 except that solid symbols are mafic tonalites (SiO_2 < 65.5 wt %). Data for tonalites and K-poor granodiorites form triangular arrays, with the mafic tonalites forming the base and the felsic differentiates the apex.

Once an horizontally extensive pool (or lens) of magma had formed, it would intercept any rising silicate liquid that reached it base, growing as it did so. More mafic liquids would be forced to crystallize on reaching the cooler magma chamber (producing the dykes, inclusions and more mafic tonalites); felsic liquids would be added to the slowly growing volume of differentiated material within the chamber, and intermediate liquids (of tonalite composition) would merely add to the increasing volume of magma of like composition and would slowly solidify as the thermal input from each new magma pulse dissipated.

Fractionation and Solidification Within the San Jacinto Plutons

The major aim of this project was to obtain data on the processes involved in the filling and solidification of these large exhumed crustal magma chambers. It was expected that the effects of these high-level processes would obscure the effects of processes operating on the silicate liquids prior to their injection into the inflating plutons. However, the realization that the compositionally variable inclusions and dyke rocks probably represent samples of these liquids [Hill, this issue] allows some inferences to be made about the earlier evolutionary history of these materials. Within the limits of the available data it appears that there is a change in the evolutionary trends for more mafic liquids at about 60 wt % SiO_2.

This difference in the apparent fractionation trend shown by the more mafic inclusions to that shown by the more felsic rocks is interpreted as resulting from differences in the fractionating phases. Within the liquids represented by the more mafic dyke rocks and inclusions, hornblende and plagioclase and perhaps quartz and ilmenite are the important early crystallizing minerals; biotite and titanite become important additional phases within the crustal magma chambers. The data for Al_2O_3 and Na_2O are suggestive of a relatively less important role for feldspar removal in the evolution of the mafic liquids (inclusions and dyke rocks); plagioclase accumulation is, however, a possibility. Trace element data are consistent with this suggestion; Sr and Ga, two elements removed during plagioclase precipitation, apparently increase in abundance until the liquids reach about 60 wt % SiO_2, at which point they begin to drop. The Cr data (Figure 5) are suggestive of removal of a Cr-rich phase early in the evolution of the more mafic liquids (SiO_2 < 60 wt %). If this phase was pyroxene, it has been completely removed from all studied samples by reaction with the evolving H_2O-rich liquids to give hornblende. Insufficient data on either liquid or mineral compositions are available to warrant detailed modeling of the evolution of these liquids prior to their injection into the observed magma chambers; however, the observations listed above suggest that most liquids injected into the magma chamber are related by initial fractionation of mafic phases (hornblende and perhaps ilmenite, pyroxene, and plagioclase), with the more evolved ones (with SiO_2 > 60 wt %) having the effects of removal of a multiphase assemblage (plagioclase + hornblende + quartz + ilmenite + biotite) superimposed.

The geochemical data are consistent with fractionation within the magma chamber involving the observed mafic phases in their observed proportions. In fact, except for K_2O (and, to a minor extent, Na_2O), the major element data define ex-

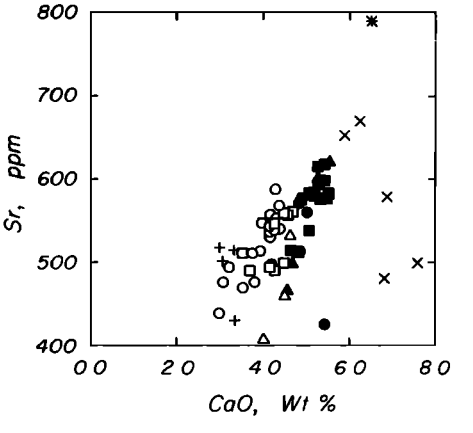

Fig. 7. CaO versus Sr. Symbols as for Figure 6. Mafic tonalites form a relatively tight linear array, felsic differentiates are displaced from this linear array, and other samples have intermediate characteristics.

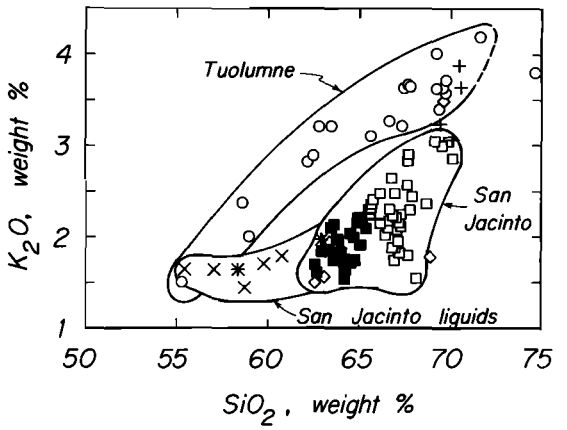

Fig. 8. Harker diagram for K_2O comparing the San Jacinto and Tuolumne intrusive complexes. Tuolumne data are from Bateman and Chappell [1979]. Biotite removal considerably restricts K enrichment for San Jacinto. San Jacinto symbols: solid squares, mafic tonalites; open squares, other tonalites and K-poor granodiorites; crosses and asterisks, inclusions and dyke rocks, respectively; diamonds, early intrusives; pluses, felsic differentiates. Tuolumne, open circles.

cellent linear arrays between the most mafic tonalites, inferred to represent largely assemblages of early crystallizing phases, and the felsic differentiates, inferred to represent the residual liquids removed from these early solidification products. The scatter of K_2O in part reflects its dependence on presence or removal of a single phase, biotite. Removal of biotite at the abundance levels of the more mafic tonalites, or of the schlieren, effectively prevents K_2O enrichment in residual liquids. Removal of only slightly less biotite than is present in the more mafic rocks allows K_2O enrichment. Two fractionation trends for K_2O are thus possible, dependent on the delicate balance between the K_2O content of a particular volume of liquid and the amount of biotite precipitated from that liquid increment.

The mafic inclusions average about 1.7 wt % K_2O; mafic tonalites are slightly more K-rich (average ≈ 1.9 wt % K_2O). A typical mafic tonalite with 15% biotite and 5% hornblende will contain 1.6 % K_2O contributed by these two early crystallizing mafic phases and an additional 0.1 % K_2O contributed by plagioclase. Removal of such a solid from the liquid resident in the magma chamber (with K_2O = 1.7-1.9 wt %) will allow K_2O in the residual liquid to increase only slowly. As the importance of biotite and hornblende declines, removal of K becomes less efficient and the K_2O content of the remaining liquid can increase more rapidly.

The removal of K by abundant early crystallizing biotite contrasts markedly with the case for the Tuolumne Intrusive Complex of the Sierra Nevada batholith (Figure 8) [Bateman and Chappell, 1979]. Here the early formed solids contain only 10-12% biotite, and biotite abundance decreases rapidly to 7% or less. By the time K-feldspar becomes a phenocrystic phase the K_2O content of the Tuolumne rocks has reached ≈3.5 wt %. K-feldspar does not become a phenocrystic phase in any of the San Jacinto major tonalite units but does occur in the small Granodiorite of Apple Canyon, which has 3.5 wt % K_2O. The bulk K_2O of San Jacinto (≈2.0-2.2 wt %) is much lower than that for Tuolumne (≈3.4-3.6 wt %). Because of this lower intrinsic K_2O content and because of the relative importance of early K-rich precipitating phases, the plutons of the San Jacinto Mountains (and the Peninsular Ranges batholith in general) cannot differentiate to yield granodiorite-dominated magmatic series like the Tuolumne Intrusive Complex (and the central Sierra Nevada batholith in general).

In summary, the simple element-element covariation shown by the more mafic rocks (SiO_2 < 65.5%), the inclusions, and the dyke rocks are interpreted as resulting from fractional crystallization of originally more mafic liquids (SiO_2 < 55%) prior to introduction of these liquids and any suspended crystals into the magma chambers. The mineralogy involved was apparently simple and included hornblende and plagioclase and perhaps a pyroxene. Once the level of the crustal magma chambers had been reached, biotite and titanite were added to the assemblage of early crystallizing phases, leading to considerable complexities in geochemical evolution dependent on the vagaries of removal of a complex assortment of phases.

The field observations [Hill, this issue] can be used to construct a model for the solidification of the eastern portion of unit III. This part of the pluton is approximately circular in plan, with outer walls dipping inward at 60-70°. Figure 9 presents a simple model of the form of this chamber as solidification proceeded. The bulk of the pluton is contained in the relatively mafic outer part; the successively shallowing inner cones hold less and less material in turn so that the inner core of K-poor granodiorite represents a minor portion of the total pluton volume. Figure 10 shows Rb and Sr concentrations within this pluton as a fraction of percentage solidified (estimated from the model). Although estimation of the percentage solidified has relatively large errors and is dependent on the exact geometry chosen, relatively simple modeling illustrates three features of this pluton:

1. There is a considerable range in both Rb and Sr abundances in marginal rocks, and in inclusions interpreted as representing samples of liquid added to the growing magma chamber.

2. Significant heterogeneity within the inclusion-rich outer part of the pluton apparently gives way at 70% solidified to a relatively restricted range of compositions from 70 to 90% solidified. This apparent change in behaviour coincides with a major inclusion train (Figure 9) interpreted as representing a zone of relative movement within the magma chamber; these trace element data suggest that this movement may have been accompanied by considerable homogenization of liquids within the chamber at this time. Strontium isotope data [Hill and Silver, this issue] demonstrate that this homogenization was not complete. This inclusion train also represents an approximate inner limit to abundant inclusion trains within this pluton, suggesting that it marks a position in the solidification history after which recharge becomes less significant, or a position sufficiently distant from the pluton base that mafic inclusions were unlikely to reach in any abundance.

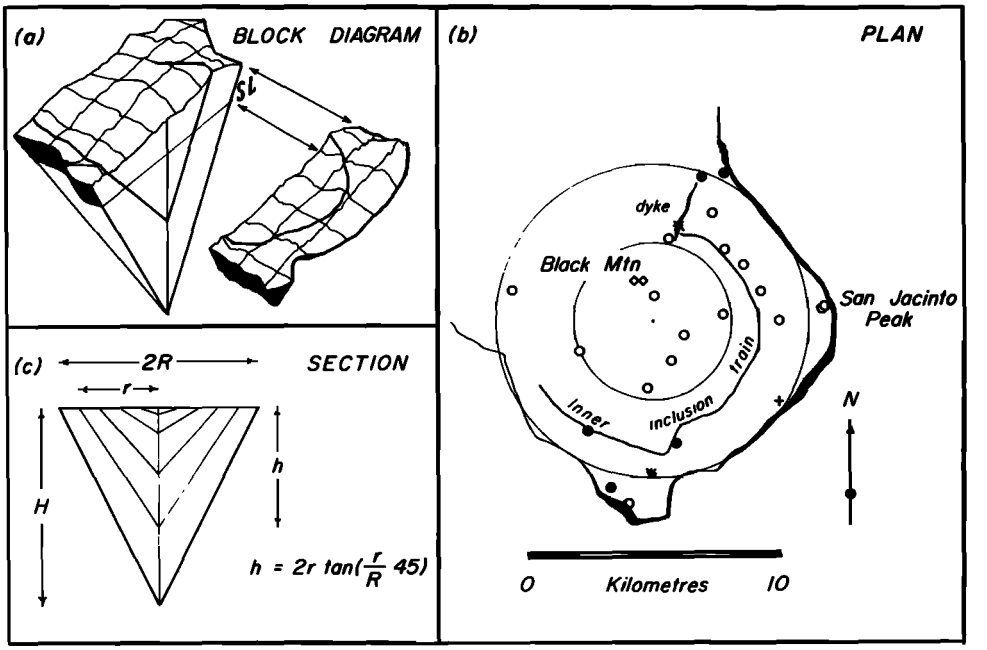

Fig. 9. Geometric model for unit III, showing solidification as a sequential series of shallowing cones. (a) Exploded block diagram showing three-dimensional configuration of eastern part of unit III extrapolated to sea level (SL) and further down dip extrapolation of contacts to give an upward opening funnel. Thick line within pluton represents major internal inclusion train. (b) Simplified map showing close approximation to circular shape, location of inner inclusion train, a major dyke, and sample locations. Inner circle is at r = 0.5. (c) Cross section showing the geometric model adopted. Cones of successively solidified material shallow inward.

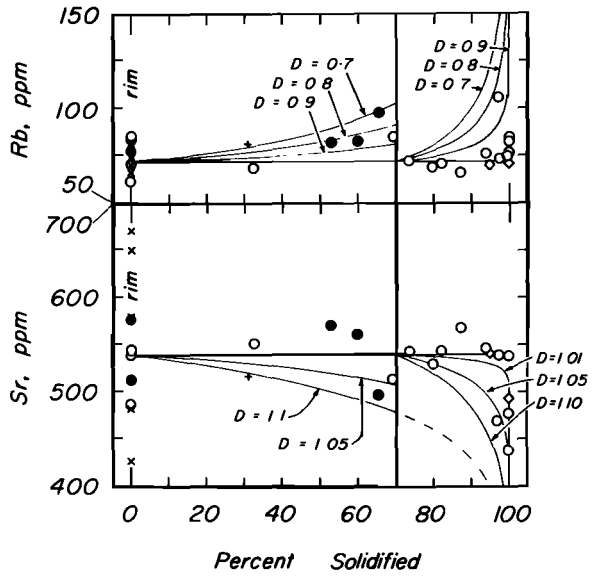

Fig. 10. Rb and Sr as a function of percentage solidified for the eastern portion of unit III. Percentage solidified from model of Figure 9. Curves give Rayleigh fractionation trajectories for labeled distribution coefficients. Solid symbols, mafic tonalites; open symbols, other tonalites and low-K granodiorites; crosses, inclusions and dyke rocks; pluses, felsic differentiate; diamonds, samples from roof zone on Black Mountain.

3. If simple Rayleigh fractionation is assumed, then both the Rb and Sr data are best modeled with $D_{solid/liq} \approx 1.0$. For a model of closed-system fractionation this implies that $D^{Rb}_{biotite/liq}$ increases from ≈ 6 to ≈ 12 exactly sympathetically with falling biotite abundance and that $D^{Sr}_{plag/liq} \approx 2$ throughout crystallization. This is thought unlikely; moreover, D ≈ 1 will allow little modification of Rb and Sr concentrations in residual liquids, and this is clearly not the case for the felsic differentiates, which have Rb = 80-100 ppm, Sr = 420-520 ppm, compared to mean values for the pluton of ≈72 ppm Rb and ≈540 ppm Sr. More complex models allow relaxation of these constraints.

Thermal and Chemical Buffering Within the Magma Chambers

Although liquids spanning a wide compositional range appear to have been added to the growing magma chamber, the end products of solidification are relatively homogeneous. This implies that the bulk of the added liquid had a restricted compositional range, that processes within the magma chamber were efficient at blending batches of different composition liquids, that solidification occurred under a restricted range of physical conditions, or that some combination of these factors was active. Trace element variation and Sr isotope heterogeneity [Hill and Silver, this issue] within the analyzed rocks provides evidence for compositional variability within the added pulses and also argue against efficient homogenization. Calculation of mean

plagioclase compositions for each rock using mineral chemical and mineral abundance data shows that the bulk plagioclase composition varies from An_{30} to An_{41} [Hill, 1984], with values $<An_{35}$ being restricted to the volumetrically minor low-K granodiorites and felsic differentiates.

Early Intrusives

The early intrusives show a much wider range of chemistry than do the major tonalites. However, with little exception, the gross geochemical features of the major tonalites are shared by the smaller, earlier bodies. The small tonalite masses tend to have lower TiO_2, Fe_2O_3, MgO, and K_2O at a given SiO_2 and slightly higher CaO and Al_2O_3. Trace element abundances follow major element patterns: Rb, Pb, V, and Cr tend to be lower in these rocks. The granodiorite of Poppet Creek is distinctive because of its high K_2O (and Rb, Pb, and Th) but also has higher MgO, Fe_2O_3, FeO, V, and Cr and lower Al_2O_3, Na_2O, P_2O_5, and Ca at a given SiO_2 than all other rocks. The K-feldspar megacryst bearing granodiorite of Apple Canyon and a felsic dyke from Thomas Mountain have, in general, the chemical characteristics of the more felsic of the major tonalites, as do samples from the granite of Penrod Canyon with the exception of lower CaO and higher Na_2O.

The granodiorite of Poppet Creek is much less plagioclase-rich than the other tonalites and K-feldspar-poor granodiorites, has an unusually high hornblende:biotite ratio of ≈1, and contains significant K-feldspar even in the most mafic rocks. This pluton also has lower Ce/Y at a given Ce than almost any other rock, implying that it has a much less fractionated rare earth element (REE) pattern. These chemical differences could result from a different source composition, from a different residual mineralogy, from different fractionating phases during ascent from the zone of partial fusion, or from some combination of these factors.

The chemical data for the early intrusives provide information on the composition of magmas reaching this level of the crust immediately prior to, and perhaps during, the filling of the large plutons. With the exception of the granodiorite of Poppet Flat all such liquids have geochemical characteristics colinear with those of the major tonalite masses. Ponding and blending of these heterogeneous but related liquids could conceivably yield a mass with the composition of the major tonalites. Although the relative areas of the different rock types are qualitatively in accord with this suggestion, more data on the relative volumes of the different compositions are needed before this can be established quantitatively.

Samples From North and East of Tahquitz Peak, and the Role of Sediment Contamination

Cropping out on the high plateau of the southern San Jacinto Mountains north from Red Tahquitz are numerous small bodies of tonalite and granodiorite. Schlieren are common and locally abundant, and comb structure is present within these heterogeneous rocks. Irregular masses of iron-rich garnet are common adjacent to contacts with enclosing metasedimentary rocks, and small garnets are observed for some distance (<100 m) from sediment/intrusive contacts, suggesting that sediment contamination may be more or less important in many of these rocks. Analyses of these samples are listed in Table 3. Only two rocks appear to be representative of "uncontaminated" undifferentiated materials on the basis of field criteria, and even these show considerable evidence for recrystallization. These two samples (293 and 314) have geochemical characteristics similar to the other rocks from the San Jacinto Mountains. Five samples show effects of sediment contamination, and are characterized by extremely low $Mg/(Mg + Fe^{2+})$, low TiO_2, variable Al_2O_3, and high Ba, Zr, and REE. The contamination process is unlikely to involve simple mixing of sediment with a tonalitic melt [e.g., Bowen, 1928; Taylor, 1980], and no attempt has been made to model the complex sequence of processes likely to have been operating. Nevertheless, the high-REE abundances in particular seem to reflect the high-REE contents of the incorporated sediments (Table 4). Three geochemical features appear characteristic of sediment incorporation: low $Mg/(Mg + Fe^{2+})$ and extremely high Zr (>350 ppm) and REE (Ce > 150x chondrites) abundances. These features are not seen in any rocks for which there is no a priori evidence for sediment incorporation.

Discussion

The detailed reexamination of crystallization and solidification within the basaltic Skaergaard Intrusion in light of advances in the understanding of rheological and physical properties of magmas [McBirney and Noyes, 1979] has stimulated much interest in studies aimed at elucidating the fluid dynamics of active magma chambers. For a calc-alkaline magma chamber, crystallization may lead to the development of a cap of less dense fractionated magma overlying relatively unmodified original liquid, with double-diffusive stratification also developing as solidification proceeds [Turner, 1980; McBirney, 1980; McBirney et al., 1985].

A further complicating factor, the rate at which the magma chamber is filled, has been considered explicitly by Huppert and Sparks [1980a,b], Huppert and Turner [1981a,b] and Huppert et al. [1983] and, from a quite different viewpoint, by O'Hara [1977, 1980] and O'Hara and Mathews [1981]. It is unlikely that a large magma chamber, such as those exposed in the San Jacinto Mountains, fills instantaneously but rather must be filled over some considerable length of time. It is difficult to estimate the rate at which such reservoirs were filled. Recent estimates of magma transport rates into volcanic systems include 0.1 $km^3\ yr^{-1}$ (or 3 $m^3\ s^{-1}$) for Kilauea [Swanson, 1972], 0.1-0.5 $m^3\ s^{-1}$ for the various volcanic centers of the Taupo Rift Zone, New Zealand [Wilson et al., 1984], and 7-5500 $m^3\ s^{-1}$ for Mount St. Helens during its 1980 eruptive phase [Scandone and Malone, 1985]. It appears unlikely that any plumbing system through which the growing magma chamber is fed would remain open for any length of time, but rather upward movement of liquid would be expected to be episodic as feeder dykes or conduits open and close in response to magmatic and lithostatic stresses. The large San Jacinto magma chambers have volumes of order 1-3 x 10^3 km^3; at magma flow rates of 1 $m^3\ s^{-1}$ these

TABLE 4. Metasedimentary Rocks

	DESERT DIVIDE GROUP						WINDY POINT METAMORPHICS			
	LTS308	LTS309	LTS310	LTS313	LTS312	LTS389	LTS386	LTS388	LTS385	LTS387
SiO_2	56.22	87.33	89.80	54.07	54.60	91.48	45.20	51.95	63.98	67.20
TiO_2	1.06	0.32	0.32	1.03	1.13	0.38	2.81	1.41	0.88	0.73
Al_2O_3	20.98	6.09	4.77	24.11	23.53	3.79	13.17	17.93	12.88	13.30
Fe_2O_3	2.17	0.26	0.34	1.76	1.73	0.09	1.21	2.25	3.25	1.64
FeO	5.38	1.19	0.94	7.13	6.59	1.00	8.34	6.60	2.05	3.25
MnO	0.07	0.02	0.02	0.07	0.07	0.01	0.14	0.19	0.08	0.05
MgO	2.37	0.42	0.36	2.81	2.51	0.28	8.85	4.30	3.21	2.16
CaO	0.22	0.86	0.54	0.49,	0.46	0.74	11.96	7.35	2.38	5.03
Na_2O	1.33	1.58	1.25	1.44	1.57	0.91	1.58	2.39	1.90	0.52
K_2O	5.10	0.77	0.55	4.67	5.25	0.43	3.37	2.33	3.90	1.79
P_2O_5	0.08	0.01	0.02	0.09	0.10	0.01	0.53	0.24	0.19	0.18
S	0.95	<0.02	<0.02	<0.02	<0.02	<0.02	<0.02	<0.02	0.03	0.28
H_2O+	1.79	0.50	0.47	1.43	1.51	0.27	1.55	1.68	1.52	1.56
H_2O-	0.70	0.13	0.09	0.32	0.38	0.06	0.19	0.39	0.41	0.50
CO_2	2.02	0.14	0.12	0.19	0.21	0.06	0.53	0.09	3.59	2.61
rest	0.27	0.12	0.09	0.27	0.30	0.11	0.29	0.26	0.53	0.34
O=S	0.47								0.01	0.14
Total	100.24	99.74	99.68	99.88	99.94	99.62	99.72	99.36	100.77	101.00
Ba	870	380	175	975	1175	140	660	920	3140	1530
Rb	129	34.5	27.5	183	193	19.0	149	67	156	81
Sr	114	78	59	119	121	60	364	530	169	386
Pb	37	7	5	6	9	5	8	8	14	9
Th	20.5	2.0	8.2	26.0	24.5	7.4	5.8	1.2	12.8	9.6
U	3.6	3.2	2.8	3.8	4.2	1.8	1.8	1.0	4.4	2.6
Zr	244	338	302	244	278	477	198	141	207	171
Nb	20.0	9.0	8.5	23.0	28.0	7.5	60	8.5	15.5	17.5
Y	46	4	8	26	43	9	27	23	17	17
La	51	5	15	55	59	18	37	11	21	21
Ce	114	14	33	118	121	53	68	31	52	47
Nb										
Sc	19	6	5	18	20	4	24	20	18	17
V	134	18	18	106	97	16	206	165	196	141
Cr	116	35	31	147	128	29	162	15	129	101
Mn	505	150	145	560	520	105	1070	1480	640	425
Ni	52	2	1	60	63	1	141	21	39	49
Cu	43	4	3	<1	2	<1	8	10	44	48
Zn	144	31	25	100	83	17	151	138	191	120
Ga	27.8	7.4	5.6	30.8	31.2	4.2	18.8	20.8	17.4	16.8

could be filled in 3-10 x 10^4 years. Periodic injection of liquid into the base of a cooling magma chamber will affect the thermal and convective regime within the chamber [e.g., Huppert and Sparks, 1980b; McBirney et al., 1985]; this may, in turn, strongly influence the solidification and fractionation history of the chamber as well (McBirney et al., 1985). The development of fractionated liquids will depend on the efficiency of separation of the liquid from crystallizing phases. Both horizontal stratification and periodic replenishment could serve to isolate volumes of magma from each other, thus enabling initial variations in either geochemical or isotopic properties to be preserved in the solidified rock.

The data presented above for the rocks of the San Jacinto Mountains enable limitations to be placed on the importance of some of these possible processes. The field data are interpreted as indicating that each magma chamber was filled by a large number of inputs of silicate liquids having a wide compositional range but dominated by liquids of tonalitic composition. The relative homogeneity of the three major tonalite units argues for some mixing of these various batches of magma, as do oxygen isotope data [Hill et al., 1986]. The consistency of mineral chemistry throughout the three major plutons argues for consistency in physico-chemical conditions during crystallization; the plagioclase data in particular appear to require considerable uniformity and stability in both the temperature and the partial pressure of water within the crystallizing liquids.

Modelling Trace Element Behaviour in Silicate Liquids

The application of trace element modeling to the elucidation of magmatic processes in isolation has been extensively reviewed by Allegre and

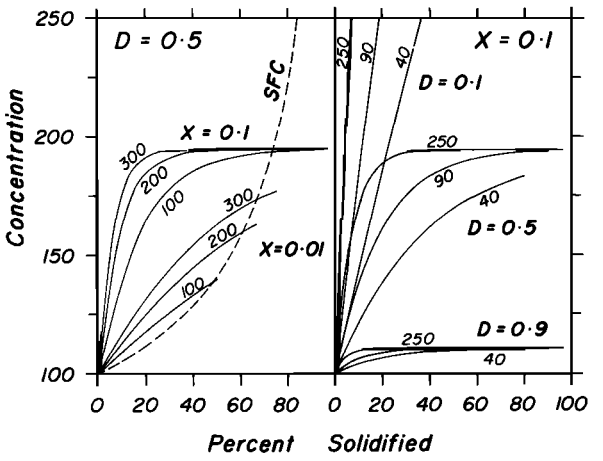

Fig. 11. Comparison showing differences between SFC and RFC processes. Solid curves give RFC trajectories for labelled values of D, X, and n. Dashed curve gives the SFC trajectory for D = 0.5.

Minster [1978] and Hanson [1978], among others. O'Hara [1977] pointed out that consideration of such simplified systems where processes are treated in isolation can lead to misleading conclusions, and Taylor [1980] has studied the isotopic, geochemical and thermal effects of one set of interactive processes, the contamination of a crystallizing (and fractionating) magma chamber. DePaolo [1981a] subsequently developed the analytical expressions that describe this process and noted explicitly that the cases of combined assimilation-fractional crystallization (AFC) and combined recharge-fractional crystallization (RFC) are mathematically similar.

Work on such interactive systems has demonstrated that these more complex and probably geologically more realistic situations yield geochemical and isotopic trajectories quite different from those obtained from simpler systems. In general, these effects are nonlinear, meaning that extrapolated trends do not necessarily pass through the composition of either end-member. DePaolo and his co-workers [DePaolo, 1981a,b; Farmer and DePaolo 1983, 1984] have demonstrated that for one simplified case (AFC) it is possible to model almost any data array by suitable variation of the model parameters. The mathematical similarity between the AFC and RFC processes thus implies that any general conclusions drawn for the AFC case must necessarily hold for the RFC case as well, with the obvious difference that the compositional and isotopic contrasts between chamber and added material will usually be much smaller for the latter (RFC) process.

The common linear element-element covariation within calc-alkaline rock suites has led many workers to suggest that mixing (or unmixing) is an important process in the generation of these rocks. It is becoming apparent that more than one process is involved in the generation of these linear relationships. Linear element covariation in southeastern Australian granites has been interpreted as resulting from the incomplete unmixing of a mafic residuum ("restite") from a more felsic granitic or granodioritic liquid [e.g., Chappell, 1966, 1978; White and Chappell, 1977; Compston and Chappell, 1979]. Linear relationships may also result from the mixing of relatively unfractionated and relatively fractionated liquids near the top of a fractionally crystallizing magma chamber [McBirney, 1980; McBirney et al., 1985; Baker and McBirney, 1985]. There appears no doubt that this mechanism can be quite efficient in developing a range of compositions within a cooling pluton, as shown by both experimental work [McBirney, 1980; McBirney et al., 1985; Turner, 1980] and by the study of exhumed natural examples [e.g., Wilcox, 1954; Bailey et al., 1976]. A variant on this process is where the felsic cap contains a significant component derived from assimilation or melting of country rocks, and mixing is between relatively mafic and felsic materials derived ultimately from quite different sources [e.g., Gerlach and Grove, 1982; Grove et al., 1982].

Combined recharge-fractional crystallization provides a third mechanism for developing rectilinear variation within a cogenetic suite of rocks. Here the mixing is between the fractionated liquid (or liquids) within the magma chamber and the new ("primitive") liquid (or liquids) being periodically added to the developing system.

These three processes need not operate in isolation; a pluton could develop a lid of less dense fractionated material at the same time as relatively dense "primitive" material is being added to the underlying liquids, and these "primitive" liquids could contain various amounts of restite, giving a final rock produced by mixing (or unmixing) at three different scales. If volumes of liquid become isolated from the bulk of the magma chamber (by double-diffusive induced stratification, by magma chamber geometry, by a hiatus in the supply of new magma, or for some other reason), then a wide and complex range of variation may be expected in the final products of igneous activity.

One important feature of the RFC process is that by continually adding new batches of "primitive" material it has the potential to buffer both the composition and physical conditions of the liquid to within a relatively narrow range. This enables a large volume of material with a narrow compositional range to crystallize from a liquid at approximately uniform temperature.

Figure 11 shows diagramatically the difference between simple closed system ("Rayleigh") fractionation (SFC) and fractionation with recharge (RFC) for the simple case where the amount of recharge exactly balances the amount solidified over any time interval. This is modeled by

$$C_n = C_{n-1}\,(1-X)^{D-1}\,(1-X) + XC_{n=0} \qquad (1)$$

where C_n is the concentration of the element in the solid (or liquid) at the nth step, X is the fraction of liquid removed (and replenished) at each stage, and D is the solid/liquid partition coefficient for the element under consideration. From Figure 11b it can be seen that if $n \gg 1/X$, then the concentration of the element in the precipitated solid (and in the residual liquid) rapidly reaches a limiting value. For this case, the volume of liquid present at any one time relative to the total final pluton volume is small; the liquid in the chamber is processed efficiently, and the steady state is soon reached. For $n \approx 1/X$, C rises slowly toward the

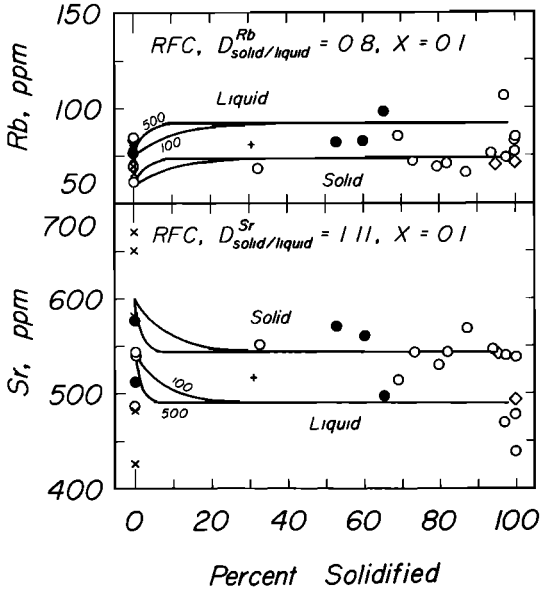

Fig. 12. RFC model for unit III. Symbols as for Figure 10. For X relatively large (≈0.1) the liquid within the chamber rapidly evolves to a relatively fractionated composition that precipitates rocks that closely match the compositions of the unfractionated added liquids. Upon cessation of recharge, the remaining fractionated liquid can further evolve to yield small volumes of highly fractionated rocks.

steady state value but will not reach it. Figure 11 illustrates also another important feature of RFC; for D ≈ 1, once steady state has been reached, then the composition of the precipitated solids matches closely that of added liquid. For example, for D = 0.5 and an initial liquid concentration of 100 ppm (of element A), the steady state solid has 97 ppm A and the steady state liquid 195 ppm A; for D = 2 and initial liquid 100 ppm, the steady state solid has 105 ppm. The correspondence between added liquid and steady state solid compositions for these examples is striking; however, the liquid from which the solid precipitates is shifted markedly in composition from the added materials.

There is a limiting value to which the RFC process can proceed (i.e., n is finite). At this point, when recharge ceases there is still evolved liquid present in the chamber, and this liquid will solidify under different conditions, perhaps by a SFC process. If the pluton fills by the addition of many small increments of liquid to a magma chamber that is small relative to the volume of the final solidified pluton, then the amount of highly fractionated liquid that can be obtained upon cessation of RFC is small. Conversely, if the pluton grows by addition of a few large increments to a large chamber, then a large amount of late, fractionated liquid can result.

A change in the concentration of an element in the recharging liquid is reflected rapidly in the concentration of that element within the magma chamber if input of the new composition is maintained. Recharge with continually variable liquids will give rise to heterogeneous solids that have a smaller compositional range than do the added heterogeneous liquids.

Application to the San Jacinto Intrusive Complex

A complete, quantitative model for solidification of the San Jacinto Intrusive Complex cannot be developed with the available data. In particular, the compositions of liquids from which the observed solids were crystallized are not well constrained, and the field evidence for periodic inputs of new magma rule out adoption of a simple closed-system fractionation model. A further possible constraint is the possibility (thought unlikely for field reasons) that substantial volumes of liquid have been lost from the system by removal (eruption) from the tops of the chambers. For the case of an RFC magma chamber, perhaps the simplest plausible case for these dynamic systems, the system is underconstrained and a unique solution impossible. Figure 12 illustrates some aspects of an RFC model for unit III. For X large and $1/X \ll n$, the concentration of an element will change markedly in the first 10-15% of rocks produced and then remain approximately constant thereafter. This contrasts markedly with the SFC case where for D≈1, the marked change in concentration occurs in the last rocks to crystallize. For example, if the steady state Sr concentration for unit III was about 540 ppm, as implied by Figure 12, then for $D_{solid/liq}$ = 1.11, the first solids to form had about 600 ppm Sr and were produced from liquids containing 540 ppm Sr. Insufficient data on marginal rock and liquid compositions are available to tell whether this is the case; however, the more mafic, presumably early solidified rocks from units I and II contain 600±20 ppm Sr, in reasonable accord with this model. This diagram further illustrates the ability of the RFC process to produce rocks that closely mimic the compositions of the liquids added to the system (though not the compositions of the liquids from which they precipitated). For this model the added liquids contain 75 ppm Rb and 540 ppm Sr; the steady state solids contain 74 ppm Rb and 544 ppm Sr, close approximations to the primary liquid compositions. This process would also act to maintain the Ca/(Ca + Na) and Mg/(Mg + Fe) of individual phases close to those of the added liquids, as is seen for minerals from the tonalites (precipitates) and the bulk composition of the inclusions and dyke rocks (representing added liquids).

In order to develop a quantitative RFC model for solidification of the San Jacinto rocks it is necessary to know the partition coefficients independently, as for any n elements the RFC equation generates n+2 unknowns if the compositions of either the evolving solids or liquids are known. However, the model developed from field observations for RFC magma chambers [Hill, this issue] appears capable of satisfying the geochemical constraints. An RFC process can produce a large volume of homogeneous rock and, by buffering the composition of the liquid in the chamber, can restrict the composition of minerals precipitated within that chamber. Finally, once recharge stops (or a portion of the chamber is isolated), solidification of the remaining evolved liquids can produce small volumes of highly fractionated materials.

Other chemical features of the major tonalite units can be explained by this model. Figure 13 shows the covariation of Ce abundance and an in-

dicator of fractionation within the REE, Ce/Y. The more mafic rocks show a linear relationship of Ce/Y with Ce; however, as the rocks become more felsic, Ce/Y increases rapidly with little variaton in Ce abundance. The triangular data array can be interpreted as resulting from mixing of "primitive" liquids having a range of Ce and Ce/Y with fractionated liquids having highly variable Ce/Y but relatively unchanged Ce. A large variation of Ce/Y within a cogenetic sequence of rocks has been suggested by Gromet and Silver [1983] to be a feature of in situ fractionation where REE behavior is controlled by minor phases (titanite, allanite, zircon), and this is precisely the situation for the San Jacinto rocks.

The K-Rb and K-U data can be interpreted similarly. The mafic rocks have K-Rb and K-U relations largely inherited from the "primitive" liquids. In situ fractional crystallization leads to high K at relatively high Rb and U, and mixing of these fractionated liquids with either less fractionated liquids or with new volumes of "primitive" liquid gives the triangular data array of Figure 6.

The effects of replenishment will depend on the frequency, relative volume, and chemical and thermal properties of each liquid increment. Frequent addition of small volumes of liquid will lead to only small variation in the chemical properties of the concurrent solid products. Significant modification of the liquid within the evolving magma chamber requires a prolonged solidification interval during which recharge is unimportant, either within an isolated portion of the chamber or for the chamber as a whole. As the supply of new magma dwindles and then ceases, crystal fractionation will eventually become the dominant petrogenetic process within the magma chamber. Homogeneous rocks produced during the RFC phase will give way inward to rocks showing evidence for solidification from chemically and thermally evolving liquids. This is seen in the central part of unit III, and to a lesser extent in units I and II. The extent to which fractionation proceeds is partly a function of liquid composition. A relatively K-poor system such as San Jacinto cannot develop a large volume of K-rich residual liquid with a relatively low solidification temperature. This is particularly the case if biotite is a major crystallizing phase from a K-poor system, effectively preventing accumulation of a K-rich residual liquid. Solidification of the bulk of the system thus takes place over a relatively restricted temperature interval, giving rise to only small variations in mineral and rock composition. In contrast, K-rich systems such as the large zoned plutons of the Sierra Nevada batholith may develop large volumes of residual liquid with a relatively low solidus temperature, and extreme fractionation may result [Bateman and Chappell, 1979; Bateman and Nokleberg, 1978]. The K-poor nature of the Peninsular Ranges batholith and the domination of the eastern part of the batholith by huge volumes of tonalite [Larsen, 1948; Silver et al., 1979) contrasts with the relatively K-rich, heterogeneous rocks of the magmatic series of the Sierra Nevada batholith [Bateman and Dodge, 1970; Presnall and Bateman, 1973; Bateman and Chappell, 1979] and reflects compositional control of the extent of fractionation. The rocks of the San Jacinto Mountains are thus seen to be an integral part of the eastern Peninsular Ranges batholith and presumably formed under similar conditions from broadly similar source rocks.

Physical Conditions Within the Magma Chambers

One of the aims of this project was the elucidation, if possible, of physical conditions within the solidifying magma chambers. Field evidence for relative movement between magma and magma chamber walls and between different volumes of magma is abundant and is described by Hill [this issue]. The estimates of magma chamber temperature (>900°C) and water content (≈3 wt %) made by comparison of the observed paragenetic sequence with those obtained experimentally [Hill, this issue], and the andesitelike composition of the mafic inclusions and tonalites allows estimation of the likely viscosity of the magmas to be $\approx 10^5$-10^7 P. These estimates allow consideration of likely fluid mechanical conditions within the magma chambers.

The Rayleigh number based on temperature is given by

$$Ra = \frac{\alpha \rho g \Delta T h^3}{\eta \kappa} \qquad (2)$$

where ΔT is the temperature difference between the cooler roof and hotter floor of a magma chamber of thickness h, α is the coefficient of thermal expansion ($\approx 5 \times 10^{-5}$ deg^{-1}), κ is the thermal diffusivity ($\approx 4 \times 10^{-3}$ cm^2 s^{-1}) η the viscosity (in poise), and ρ and g are density and acceleration due to gravity, respectively. For the San Jacinto magma chambers, h is large (10^5 cm or greater) and dominates the relationship; Ra is large (order 10^{10} or greater).

Ra specifically considers the effects of density-driven instability related to the effects of an imposed thermal gradient. A superimposed chemical gradient may also produce a density gradient within a body of fluid. The effect of this may be to either stabilize or to destabilize a system with a concurrent temperature-induced density gradient, depending on the particular case. A Rayleigh number based on density difference can be defined [Richter and McKenzie, 1981]

$$R\rho = \frac{g\rho(\Delta\rho/\rho)h^3}{\eta \kappa} \qquad (3)$$

where $\Delta\rho$ is the (compositionally induced) density contrast over distance h and ρ is the mean density of the system.

If a compositionally induced upward decrease in density is insufficient to balance a downward decrease in density related to a temperature gradient (thermal expansion), the system is unstable. The ratio $Ra/R\rho$ [$=\alpha\Delta T(\rho/\Delta\rho)$] thus gives an indication of the relative importance of temperature versus chemically induced density gradients. Richter and Johnson [1974] suggest that if $Ra > \approx 10^4$, the likely case for the San Jacinto plutons, then the system will convect regardless of the value of $R\rho$. If (for $Ra > 10^4$) $R\rho > Ra$, then the system is likely to be broken into a series of layers with convection taking place within each layer; if $Ra > R\rho$, then the whole system (of thickness h) will convect [Richter and McKenzie, 1981]. Because of the magnitude of α ($\approx 5 \times 10^{-5}$), $R\rho > Ra$ is the expected case within a magma chamber unless ΔT is unusually large or $\Delta\rho$ effectively zero. This implies that layered convection is expected to be the normal case within

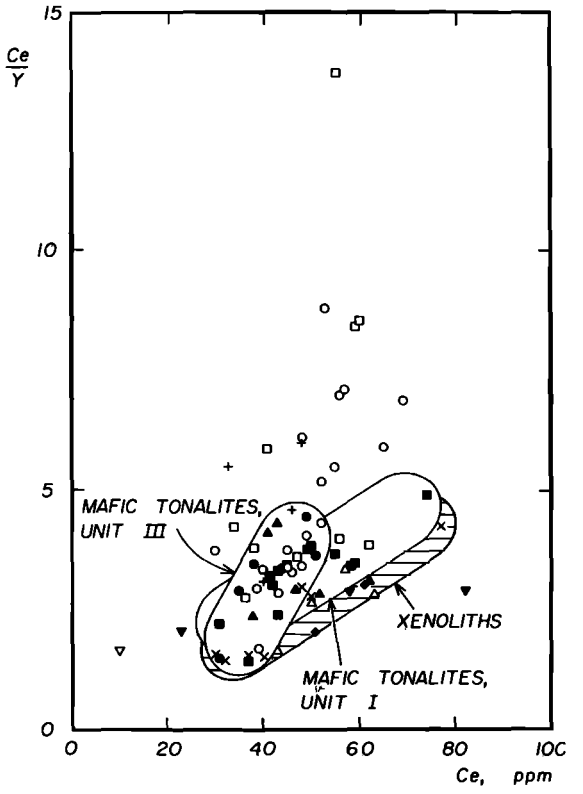

Fig. 13. Ce/Y versus Ce for San Jacinto rocks and inclusions. Data form triangular array interpreted as mixing between liquids giving mafic tonalites and variably fractionated felsic differentiate-like liquids. Large range in Ce/Y is predicted for systems where REE behavior is controlled by precipitation of accessory phases (allanite, titanite, zircon) [Gromet and Silver, 1983].

a large, low-yield-strength-liquid-containing crustal magma chamber. Note that the ratio $Ra/R\rho$ is independent of both h (magma chamber height) and η (liquid viscosity).

The consistency of mineral compositions throughout the crystallization history of the San Jacinto liquids suggests that there were not large long-lived temperature gradients within the magma chambers. It is more difficult to estimate the magnitude of $\Delta\rho$. Rocks within unit III certainly become less dense inward and upward, but whether this situation also occurred while the magmas were still liquid cannot be ascertained. Residual liquids developed during crystallization at the inward sloping walls would rise upward, giving a mechanism for developing a density gradient within the overlying liquids. The available field data are inadequate to determine the nature of convection within the magma chamber, other than to suggest that it may have been complex and variable.

Rapidly increasing yield strength within a multiply-saturated crystal-rich magma would tend to damp out convective behavior as crystallization proceeds. Viscosity of the magma will also increase as crystallization proceeds but would need to increase to some 10^{10}-10^{11} P before this factor alone would inhibit convection within a magma chamber of considerably vertical dimensions (1 km or more) and with even a small superimposed temperature gradient (10°C).

Any convective pattern is likely to have been influenced by the shapes of the magma chambers. In unit III, in particular, the thin "wings" of the chamber edges would probably be quite effective in isolating less than whole-pluton-scale convective cells from each other, even within a rapidly overturning system.

Conclusions

1. The bulk of the igneous rocks of the San Jacinto Intrusive Complex have a limited range of chemistry. SiO_2 for the majority of rocks is between 63 and 68 wt %. Over 60% of samples from units I and II have between 63 and 65 wt % SiO_2; 60% of samples from unit III fall in the restricted range $66.5 < SiO_2 < 68.0$). Liquids being added to the magma chambers spanned at least the compositional range from 55 to 66 wt % SiO_2; liquids of tonalite composition, however, appear to have predominated. Addition of new volumes of magma buffered both chemical and thermal conditions within the magma chambers. The homogeneous nature of vast volumes of rock is interpreted as indicating that there must have been considerable mixing of these added materials into the liquids already resident in the magma chamber. Oxygen isotope data [Hill et al., 1986] are consistent with this conclusion.

2. There appears to be a dichotomy between the composition of the mafic tonalites ($62.5 < SiO_2 < 65.5$) and the more chemically evolved felsic tonalites ($SiO_2 > 68$) and minor granodiorites of the major plutons. Other tonalites have intermediate properties. The mafic tonalites show linear interelement covariation for all elements. The most felsic rocks have field and geochemical characteristics consistent with derivation by fractional crystallization processes involving the observed mineral assemblage. This dichotomy appears to result from the operation of processes at different stages in the evolution of these systems. The more mafic rocks are interpreted as having crystallized from liquids that had largely acquired their geochemical characteristics prior to introduction into the relatively high-level magma chambers, while the most felsic rocks are interpreted as having crystallized from liquids that had undergone considerable chemical evolution within the magma chamber. Many of the chemical features of the San Jacinto rocks can be interpreted as having resulted from mixing of these two types of genetically related liquids within a dynamic magma chamber.

3. Aspects of trace element characteristics of these rocks (K-Rb, K-U, Ce-Ce/Y) are compatible with an RFC (recharge-fractional crystallization) process operating within a dynamic magma chamber. An RFC process is also capable of explaining the correspondence of tonalite (precipitate) and inclusion (liquid) compositions; for $D \approx 1$, precipitated solids mimic closely the geochemical characteristics of added liquids.

4. The thermal Rayleigh number for these bodies early in their crystallization histories is estimated to be $>10^{10}$. The implication is that the liquids within the magma chamber were convecting, at least throughout the early stages of inflation and solidification. This is consis-

tent with field evidence for fluid flow within the magma chambers and the evidence for mixing new, added liquids with those resident in the magma chamber. It is not possible to determine whether convection involved the whole chamber or was restricted to narrow, horizontally extensive layers (perhaps double-diffusively induced layering). Both may have occurred.

Acknowledgements. This work was conducted as part of a Ph.D. project supervised by L.T.S. Funding was provided by a Conoco Fellowship, by the Division of Geological and Planetary Sciences, California Institute of Technology, and by the Australian Research Grants Committee. This work has benefited from discussion with many people, but particularly Dave Walker, Steve Sparks, Alex McBirney, Wes Hildreth and Mike Dungan. Dungan pointed out the need for a model that explained the similarity of (inferred) liquid and solid Na/(Na+Ca) and Mg(Mg/Fe) ("Dungan's Dilemna"). Journal reviews by Calvin Barnes and Lawford Anderson led to significant improvements in clarity. Division of Geological and Planetary Sciences, California Institute of Technology, contribution 4161.

References

Allegre, C.J., and J.F. Minster, Quantitative models of trace element behaviour, Earth. Planet. Sci. Lett., 38, 1-25, 1978.

Bailey, R.A., G.B. Dalrymple, and M.A. Lanphere, Volcanism, structure and geochronology of Long Valley Caldera, Mono County, California, J. Geophys. Res., 81, 725-744, 1976.

Baker, B.H., and A.R. McBirney, Liquid Fractionation, part III: Geochemistry of zoned magmas and the compositional effects of liquid fractionation, J. Volcanol. Geotherm. Res., 24, 55-81, 1985.

Bateman, P.C., and B.W. Chappell, Crystallization, fractionation and solidification of the Tuolumne intrusive series, Yosemite National Park, California, Geol. Soc. Am. Bull., 90, 465-482, 1979.

Bateman, P.C., and F.C.W. Dodge, Variations of major chemical constituents across the central Sierra Nevada batholith, Geol. Soc. Am. Bull., 81, 409-420, 1970.

Bateman, P.C., and W.J. Nokleberg, Solidification of the Mount Givens Granodiorite, Sierra Nevada, California, J. Geol., 86, 563-579, 1978.

Bowen, N.L., Evolution of the Igneous Rocks, Princeton University Press, Princeton, N.J., 1928.

Burnham, C.W., Magmas and hydrothermal fluids, in, Geochemistry of Hydrothermal Ore Deposits, 2nd ed., edited by H.L. Barnes, pp. 71-136, John Wiley, New York, 1979.

Chappell, B.W., Petrogenesis of the granites at Moonbi, New South Wales, Ph.D. thesis, Aust. Natl. Univ., Canberra, 1966.

Chappell, B.W., Granitoids from the Moonbi district, New England Batholith, eastern Australia, J. Geol. Soc. Aust., 25, 267-283, 1978.

Chappell, B.W., and A.J.R. White, Two contrasting granite types, Pac. Geol., 8, 173-174, 1974.

Collins, W.J., S.J. Beams, A.J.R. White, and B.W. Chappell, Nature and origin of A-type granites with particular reference to southeastern Australia, Contrib. Mineral. Petrol., 80, 189-200, 1982.

Compston, W., and B.W. Chappell, Sr-isotope evolution of granitoid source rocks, The Earth: Its Origin, Structure, and Evolution, edited by M.W. McElhinny, pp. 477-476, Academic, Orlando, Fla., 1979.

DePaolo, D.J., Trace element and isotopic effects of combined wallrock assimilation and fractional crystallization, Earth Planet. Sci. Lett., 53, 189-202, 1981a.

DePaolo, D.J., A neodymium and strontium isotopic study of the Mesozoic calc-alkaline granitic batholiths of the Sierra Nevada and Peninsular Ranges, California, J. Geophys. Res., 86, 10,470-10,488, 1981b.

Farmer, G.L., and D.J. DePaolo, Origin of Mesozoic and Tertiary granite in the western United States and implications for pre-Mesozoic crustal structure, 1, Nd and Sr isotopic studies in the geosyncline of the northern Great Basin, J. Geophys. Res., 88, 3379-3402, 1983.

Farmer, G.L., and D.J. DePaolo, Origin of Mesozoic and Tertiary granite in the western United States and implications for pre-Mesozoic crustal structure, 2, Nd and Sr isotopic studies of unmineralized and Cu- and Mo-mineralized granite in the Precambrian craton, J. Geophys. Res., 89, 10,141-10,160, 1984.

Gerlach, D.C., and T.L. Grove, Petrology of Medicine Lake Highland volcanics, Characterization of end-members of magma mixing, Contrib. Mineral. Petrol., 80, 147-159, 1982.

Gill, J., Orogenic Andesites and Plate Tectonics, 390 pp., Springer-Verlag, New York, 1981.

Gromet, L.P., and L.T. Silver, Rare earth element distributions among minerals in a granodiorite and their petrogenetic implications, Geochim. Cosmochim. Acta, 47, 925-939, 1983.

Grove, T.L., D.C. Gerlach, and T.W. Sando, Origin of calc-alkaline series lavas at Medicine Lake Volcano by fractionation, assimilation and magma mixing, Contrib. Mineral. Petrol., 80, 160-182, 1982.

Hanson, G.N., The application of trace elements to the petrogenesis of igneous rocks of granitic composition, Earth Planet. Sci. Lett., 38, 26-43, 1978.

Hill, R.I., Petrology and petrogenesis of batholithic rocks, San Jacinto Mountains, southern California. Ph.D. thesis, 660 pp., Calif. Inst. of Technol., Pasadena, 1984.

Hill, R.I., San Jacinto Intrusive Complex, 1, Geology and mineral chemistry and a model for intermittent recharge of tonalitic magma chambers. J. Geophys. Res., this issue.

Hill, R.I., and L.T. Silver, San Jacinto Intrusive Complex, 3, Constraints on crustal magma chamber processes from strontium isotope heterogeneity, J. Geophys. Res., this issue.

Hill, R.I., L.T. Silver, B.W. Chappell, and H.P. Taylor, Jr., Solidification and recharge of SiO_2-rich plutonic magma chambers, Nature, 313, 643-646, 1985.

Hill, R.I., L.T. Silver, and H.P. Taylor, Jr., Coupled Sr-O isotope variations as an indicator of source heterogeneity for the northern Peninsular Ranges batholith, Contrib. Mineral. Petrol., 92, 351-361 1986.

Huppert, H.E., and R.S.J. Sparks, The fluid dyna-

mics of a basaltic magma chamber replenished by influx of hot, dense ultrabasic magma, Contrib. Mineral. Petrol., 75, 279-289, 1980a.

Huppert, H.E., and R.S.J. Sparks, Restrictions of the compositions of mid-ocean ridge basalts: A fluid dynamical investigation, Nature, 286, 46-48, 1980b.

Huppert, H.E., and J.S. Turner, Double-diffusive convection, J. Fluid Mech., 106, 299-329, 1981a.

Huppert, H.E., and J.S. Turner, A laboratory model of a replenished magma chamber, Earth Planet. Sci. Lett., 54, 144-172, 1981b.

Huppert, H.E., R.S.J. Sparks, and J.S. Turner, Laboratory investigations of viscous effects in replenished magma chambers, Earth Planet. Sci. Lett., 65, 377-381, 1983.

Larsen, E.S., Jr., Batholith and associated rocks of Corona, Elsinore, and San Luis Rey quadrangles, southern California, Mem. Geol. Soc. Am., 29, 182 pp., 1948.

McBirney, A.R., Mixing and unmixing of magmas, J. Volcanol. Geotherm. Res., 7, 357-371, 1980.

McBirney, A.R., and R.M. Noyes, Crystallization and layering of the Skaergaard intrusion, J. Petrol., 20, 487-554, 1979.

McBirney, A.R., B.H. Baker, and R.H. Nilson, Liquid fractionation, part I, Basic principles and experimental simulations, J. Volcanol. Geotherm. Res., 24, 1-24, 1985.

Norrish, K., and Chappell, B.W., X-ray flourescence spectrometry, Physical Methods in Determinative Mineralogy, 2nd edition, edited by J. Zussman, pp. 201-272, Academic Press, London, 1977.

Norrish, K., and Hutton, J.T., An accurate x-ray spectrographic method for the analysis of a wide range of geological samples, Geochim. Cosmochim. Acta, 33, 431-453, 1969.

O'Hara, M.J., Geochemical evolution during fractional crystallization of a periodically refilled magma chamber, Nature, 266, 503-507, 1977.

O'Hara, M.J., Nonlinear nature of the unavoidable long-lived isotopic, trace and major element contamination of a developing magma chamber, Philos. Trans. Soc. London, Ser. A, 297, 215-227, 1980.

O'Hara, M.J. and R.E. Mathews, Geochemical evolution in an advancing, periodically replenished, periodically tapped, continously fractionated magma chamber, J. Geol. Soc. London, 138, 237-277, 1981.

Presnall, D.C., and P.C. Bateman, Fusion relationships in the system $NaAlSi_3O_8$-$CaAl_2Si_2O_8$-$KAlSi_3O_8$-SiO_2-H_2O and generation of granitic magmas in the Sierra Nevada Batholith, Geol. Soc. Am. Bull., 84, 3181-3202, 1973.

Richter, F.M., and C.E. Johnson, Stability of a chemically layered mantle, J. Geophys. Res., 79, 1635-1639, 1974.

Richter, F.M., and D.P. McKenzie, On some consequences and possible causes of layered mantle convection, J. Geophys. Res., 86, 6133-6142, 1981.

Scandone, R., and S.D. Malone, Magma supply, magma discharge and readjustment of the feeding system of Mount St. Helens during 1980, J. Volcanol. Geotherm. Res., 23, 239-262, 1985.

Silver, L.T., H.P. Taylor, Jr., and B.W. Chappell, Some petrological, geochemical and gechronological observations of the Peninsular Ranges batholith near the International border of the U.S.A. and Mexico, Mesozoic Crystalline Rocks, Manuscripts and Road Logs Prepared for the Geological Society of America Annual Meeting, San Diego., edited by P.L. Abbott and V.R. Todd, pp. 83-110, Department of Geological Sciences, San Diego State University, San Diego, Calif., 1979.

Swanson, D.A., Magma supply rate at Kilauea Volcano, 1952-1971, Science, 175, 169-170, 1972.

Taylor, H.P., Jr., The effects of assimilation of country rocks by magmas on $^{18}O/^{16}O$ and $^{87}Sr/^{86}Sr$ systematics in igneous rocks, Earth Planet. Sci. Lett., 47, 243-254, 1980.

Turner, J.S., A fluid dynamical model of differentiation and layering in magma chambers, Nature, 285, 213-215, 1980.

White, A.J.R., and B.W. Chappell, Ultrametamorphism and granitoid genesis, Tectonophysics, 43, 7-22, 1977.

Wilcox, R.E., Petrology of Paricutin Volcano, Mexico, U.S. Geol. Surv. Bull., 965-C, 281-353, 1954.

Wilson, C.J.N., A.M. Rogan, I.E.M. Smith, D.J. Northey, I.A. Nairn, and B.F. Houghton, Caldera volcanoes of the Taupo Volcanic Zone, New Zealand, J. Geophys. Res., 89, 8463-8484, 1984.

B. W. Chappell, Geology Department, Australian National University, P.O. Box 4, Canberra 2600, Australia.

R. I. Hill, Research School of Earth Sciences, Australian National University, Institute of Advanced Studies, P.O. Box 4, Canberra 2601, Australia.

L. T. Silver, Division of Geological and Planetary Sciences, California Institute of Technology, Pasadena, CA 91125

(Received November 26, 1984;
revised March 3, 1986;
accepted March 4, 1986.)